Manuscript Details

Manuscript number JPLPH_2018_374

Title Origanum vulgare essential oils inhibit glutamate and aspartate metabolism altering the photorespiratory pathway in Arabidopsis thaliana seedlings

Abstract

Essential oils (EOs) have been extensively studied as valuable eco-friendly compounds, with herbicidal activity, for weed management. Phytotoxic potential of EOs, extracted from a wild population of Origanum vulgare ssp. hirtum (Link) letswaart, has been here evaluated on plant model Arabidopsis, through a physiological and metabolomic approach. The EOs composition was mainly characterized by monoterpenes and sesquiterpenes, with a strong abundance of two monoterpenic phenols, namely carvacrol and thymol, and the monoterpene o-cymene. The in-vitro bioassay confirmed a strong phytotoxic effect of EOs on Arabidopsis rosettes, showing by both a strong growth reduction and highly chlorotic leaves. In well-developed seedlings, EOs firstly caused growth reduction and leaf chlorosis, together with a series of interconnected metabolic alterations: i) impairing the nitrogen assimilation into amino acids, which affects in particular the glutamine metabolism; and as consequence ii) excessive accumulation of toxic ammonia into the leaves, associated with oxidative stress and damage; iii) declining the efficiency of the photosynthetic apparatus, connected to the reduced CO2 fixation and photooxidation protection; iv) impairing the photorespiratory pathway. Overall, the results highlights that EOs alters principally the ability of Arabidopsis seedlings to incorporate inorganic nitrogen into amino acids, principally glutamine, leading to a dramatic accumulation of ammonia in leaf cells. This primary effect induces, in turn, a cascade of reactions that limits the efficiency of PSII, inducing oxidative stress and finally causing a strong plant growth reduction, leaf necrosis and eventually plant death.

Submission Files Included in this PDF

File Name [File Type]

Manuscript-30-08-18.docx [Manuscript File]

Figure 1.JPG [Figure]

Figure 2.jpg [Figure]

Figure 3.tif [Figure]

Figure 4.tif [Figure]

Figure 5.tif [Figure]

Figure 6.tif [Figure]

Figure 7.tif [Figure]

Figure 8.tif [Figure]

Figure 9.tif [Figure]

Figure 10.tif [Figure]

To view all the submission files, including those not included in the PDF, click on the manuscript title on your EVISE Homepage, then click 'Download zip file'.

Origanum vulgare essential oils inhibit glutamate and aspartate metabolism altering the photorespiratory pathway in *Arabidopsis thaliana* seedlings

Araniti F.[1,§,*], Landi M.[2§], Lupini A.[1], Sunseri F.[1], Guidi L.[2] and Abenavoli M.R.[1]

[1]Dipartimento AGRARIA, Università Mediterranea di Reggio Calabria, – Località Feo di Vito, SNC I-89124 Reggio Calabria RC, Italy

[2]Department of Agriculture, Food and Environment, University of Pisa, Pisa, Italy

[§] These authors equally contributed to the manuscript.

Corresponding author:

Fabrizio Araniti

Dipartimento di AGRARIA

Università degli Studi "Mediterranea" di Reggio Calabria

I-89122 Località Feo di Vito – Reggio Calabria, Italia

e-mail: fabrizio.araniti@unirc.it

Abstract

Essential oils (EOs) have been extensively studied as valuable eco-friendly compounds, with herbicidal activity, for weed management. Phytotoxic potential of EOs, extracted from a wild population of *Origanum vulgare* ssp. *hirtum* (Link) Ietswaart, has been here evaluated on plant model Arabidopsis, through a physiological and metabolomic approach. The EOs composition was mainly characterized by monoterpenes and sesquiterpenes, with a strong abundance of two monoterpenic phenols, namely carvacrol and thymol, and the monoterpene *o*-cymene. The *in-vitro* bioassay confirmed a strong phytotoxic effect of EOs on *Arabidopsis* rosettes, showing by both a strong growth reduction and highly chlorotic leaves. In well-developed seedlings, EOs firstly caused growth reduction and leaf chlorosis, together with a series of interconnected metabolic alterations: i) impairing the nitrogen assimilation into amino acids, which affects in particular the glutamine metabolism; and as consequence ii) excessive accumulation of toxic ammonia into the leaves, associated with oxidative stress and damage; iii) declining the efficiency of the photosynthetic apparatus, connected to the reduced CO_2 fixation and photooxidation protection; iv) impairing the photorespiratory pathway. Overall, the results highlights that EOs alters principally the ability of *Arabidopsis* seedlings to incorporate inorganic nitrogen into amino acids, principally glutamine, leading to a dramatic accumulation of ammonia in leaf cells. This primary effect induces, in turn, a cascade of reactions that limits the efficiency of PSII, inducing oxidative stress and finally causing a strong plant growth reduction, leaf necrosis and eventually plant death.

Keywords: metabolomic; essential oils; phytotoxicity; nitrogen metabolism; photosynthesis; volatiles

INTRODUCTION

Nowadays, the negative effects of synthetic herbicides to human health and environment is regarded as a real problem (Aktar et al., 2009). As a result, in the last years, the research has been focused on exploring for new eco-friendly compounds, with herbicidal activity, for crop protection and weed management (Dayan et al., 2009). Among natural products, essential oils (EOs) are very promising substances, exhibiting a wide range of biological activities and already proficiently used in agriculture as fungicides (Isman, 2000), insecticides (Khani and Asghari 2012) and nematicidal products (Andrés et al. 2012). Recently, a major attention has been also paid to EOs chemical characterization and their

phytotoxic potential extracted from different species (Garcia-Rellan et al., 2016; Araniti et al., 2013a,b; Verdeguer et al., 2016; Tworkoski 2002; Rolli et al., 2014). A large number of allelochemicals, principally belonging to the terpenoids family, has been identifiedand tested for their phytotoxicity in EOs (Araniti et al., 2016; Araniti et al., 2017a; Araniti et al., 2017b; Graña et al., 2013). Interestingly, they pointed out a wide range of metabolic targets (Chaimovitsh et al. 2010; Duke et al. 2004) such as chlorophyll synthesis and photosynthesis (De Feo, 2002). Among them, both the monoterpene citral and the sesquiterpene farnesene are able to alter hormonal balance and cell ultrastructure in seedlings of *Arabidopsis thaliana* (Araniti et al. 2017a; Araniti et al. 2016; Graña et al. 2016). Furthermore, both the sesquiterpene *trans*-caryophyllene and the monoterpene citral alter the plant water status inhibiting the germination and growth of several weeds (Araniti et al. 2017b; Graña et al. 2016), whereas the monoterpene 1,8-cineole strongly inhibits all the mitosis phases and the respiration of isolated organelles (Romagni et al. 2000). The high variety of combinations of different terpenoids, with diverse biological activity, in EOs composition, could be really interesting to develop new multi-targeted bio-herbicides as it allows: 1) the synergistic interaction among their components, increasing the biological activity (Araniti et al. 2013a; Andrés et al., 2017); 2) the trigger of phytotoxic activity of compounds present at non-phytotoxic concentration and/or sometimes in traces (Araniti et al. 2013a); 3) the overcome of resistance phenomenon to the synthetic herbicides (Vrbničanin et al. 2017). As reported by Holt et al. (1993), the classes of herbicides against which resistance is largely increasing tend to have single target sites under the control of single or very few genes.

However, despite the increasing interest in EOs and/or in their isolated constituents as natural herbicides for weed management, the studies have been focused on the effects on germination process, seedlings growth of weeds and crops (Amri et al., 2013) but little information deepened on their impact on plant metabolism and/or on the metabolic pathway affected. For example, many studies have referenced on the phytotoxic potential of *Origanum* ssp. EOs and their volatile compounds on germination and seedlings growth of weeds and crops (Atak et al., 2016; Amri et al., 2013; De Almeida et al., 2010; Dadalio□lu and Evrendilek, 2004; Dudai et al., 1999).

Therefore, the aim of the present study is to evaluate the phytotoxic potential of the EOs extracted from a wild population of *Origanum vulgare* ssp. *hirtum* (Link) Ietswaart in order to identify their mode of action and metabolic targets through a

physiological and metabolomic approach. A particular attention is focused on their effects on the photosynthetic machinery.

MATERIALS AND METHODS

Plant collection, essential oil extraction and chemical characterization

Plant collection and distillation

Aerial parts of a Calabrian wild population of *O. vulgare* L. ssp. *hirtum* were collected on July, at the beginning of the flowering stage (balsamic period), in the locality of Podargoni (RC) (southern Italy, 38°09'47.5"N 15°46'43.5"E) and immediately processed. Essential oils (EOs) were extracted using a semi-industrial stainless-steel distilling apparatus. Samples were distilled for four hours and the obtained oils were separated from the hydrolates, dried with anhydrous sodium sulphate and stored in dark vials at -20 °C.

GC-MS analysis

Essential oils (EOs) were chemically characterized using a Thermo Fisher (Waltham, Massachusetts, US) gas chromatograph apparatus (Trace 1310) equipped with a single quadrupole mass spectrometer (ISQ LT). The capillary column was a TG-5MS 30 m×0.25 mm×0.25µm, the gas carrier was helium with a flow of 1 mL/min. Injector and source temperatures were settled at 200 °C and 260 °C, respectively. Sample was diluted 1:100 (v:v) in ethanol and 1µl was injected in a split mode with a split ratio of 60. The programmed temperature was as follow: isocratic for 3 minutes 60 °C for, from 60 °C to 240 °C with a rate of 3 °C per min then isocratic for 4 minutes at 240 °C. Mass spectra were recorded in electronic impact (EI) mode at 70 eV, scanning the 40–400 m/z range. Compounds identification was carried out comparing the relative retention time and mass spectra of the molecules with those of the libraries (NIST, mainlib, wiley8, wiley fragrances etc.).

In-vitro bioassays

Seeds of *Arabidopsis thaliana* (L.) Heynh., ecotype Columbia (Col-0), were surface sterilized and vernalized as reported by Araniti et al. (2017b). Sterilized seeds were sown in square Petri dishes (100 x 100 mm) containing agar (0.8 % agar w/v) medium enriched

with a mixture of micro- and macronutrients (Murashige-Skoog, Sigma-Aldrich SRL, Milan, Italy) supplemented with 1% sucrose (w/w). Plates, placed horizontally to encourage rosette growth, were transferred in a growth chamber at 22 ± 2 °C and light intensity of 90 mol m^{-2} s^{-1} supplied by a cool white fluorescent lamp (Polylux XL FT8, 55W 8440). After germination, ten uniform seedlings (4-days-old) were transferred to a single plate and grown for 10 days with same medium containing 0, 8, 16, 32, 64, 125, 250, 500 µL/L EOs, which were previously dissolved in ethanol (0.1% v/v). The same amount of ethanol was added to the control plates. At the end of EOs treatment, the aerial parts were collected and weighted (FW, g). A dose-response curve of FW to increasing EOs concentrations allowed us to determine the ED_{50} value (dose causing 50% inhibition of the total response) to be used for all the subsequent experiments.

Chlorophyll *a* fluorescence parameters

Arabidopsis seedlings (8-days-old) were treated for 10 days with 110.91 µL/L EOs and the chlorophyll *a* fluorescence emitted was monitored every two days for 10 days using the Maxi-Imaging-PAM Chlorophyll Fluorescence System fluorometer (Walz, Effeltrich, Germany), as previously described by Araniti *et al.* (2017c). The maximum efficiency of photosystem II (PSII) in dark-adapted state (F_v/F_m), the effective PSII photochemical quantum yield (Φ_{II}), the quantum yield of regulated (Φ_{NPQ}) and non-regulated non-photochemical energy loss in PS II (Φ_{NO}), the non-photochemical quenching coefficient (q_N); the fraction of open PS II reaction centers based on a lake model (q_L) were evaluated.

Photosynthetic response was monitored for 5 min, and fifteen measurements were obtained for each parameter at each measuring time.

Fresh weight (FW), dry weight (DW), DW/FW, pigments content, total protein content and lipid peroxidation

Immediately after treatment, a bunch of 10 seedlings (18-days-old) were pulled together (considered as a replicate) and weighted (FW). Samples were then oven-dried at 60 °C for 48 h for DW determination. Pigment content (chlorophyll *a*, chlorophyll *b* and total carotenoids) and lipid peroxidation were evaluated as previously reported by Araniti et al. (2017b). In particular, pigments content was calculated using Wellburn's equations

(Wellburn, 1994), whereas lipid peroxidation using Hodges's equations (Hodges et al., 1999) with some modifications (Landi, 2017). Total protein content was evaluated using the Bradford method (Bradford, 1976)

In-situ semi-quantitative determination of H_2O_2

Hydrogen peroxide was determined as reported by Araniti et al. (2017c) following a modified version of the Van Acker et al. method (2000). After EOs treatment, rosettes, separated from roots, were vacuum infiltrated for 5min with 1 mg/mL solution of 3,3-diaminobenzidine (DAB) (pH 3.8). Successively, they were incubated in the previously described solution for 8 h in dark conditions at room temperature. After incubation, rosettes were exposed to sun light for 15 min, washed in 96% EtOH till chlorophyll pigments were completely removed and fixed in 70% glycerol. An image of the stained rosettes was captured using a camera (Canon EOS 30D).

Leaf stomatal density and size

Leaf stomatal density, expressed as stomata number per unit leaf area (Radoglou and Jarvis, 1990), was evaluated. Detached leaves were firstly cleaned using a degreased cotton ball, placed on microscope slides, wetted with few drops of 1:1 solution of phosphate buffer saline (pH 7) and pure glycerol and then covered with a cover slip.
Stomata number for each sample was counted under an epifluorescence microscope system (Olympus bx53, Shinjuku, Tokyo, Japan) and stomatal density was obtained by dividing the stomata number to the surface unit. Stomatal size, which might indicate the maximum potential opening of the stomatal pore, but not the aperture of opening that actually occurs, was defined as the length in micrometers between the junctions of the guard cells at each end of the stoma (Malone et al., 1993; Maherali et al., 2002).

Impact of essential oils on plant metabolism

To evaluate the EOs impact on plant metabolome, untreated and treated rosettes were collected and the metabolome was extracted and derivatized as previously described by Araniti et al. (2017c). The derivatized extract (1 μL) was injected in splitless mode (flow

of 1 mL/min) into a TG-5MS capillary column with injector and detector settled at the temperature of 250 °C and 260 °C, respectively. Compound separation was achieved using the following programmed temperature: isothermal 5 min at 70 °C followed by a 5 °C/ min ramp to 350 °C and a final 5min heating at 330 °C. Mass spectra were recorded in electronic impact (EI) mode at 70 eV, scanning at 45–500 m/z range.
Plant metabolites were identified using mass spectral libraries (NIST 2005, Wiley 7.0 etc.). Relative metabolites quantification was based on internal standard (ribitol 0.02 mg/mL) added during the extraction process.

Ionomic analysis

Ion chromatography was employed to evaluate the variation in cations content in seedlings (8-days-old) treated for 10 days with the 110.9 µL/L EOs. A pool of 40 seedlings were collected, dried at 60 °C, weighted and finally reduced to ashes at 550 °C for 12 hours. A known amount of ashes (the equivalent of one gram of dry plant material) was digested in 20 mL of HCl 1M at 100 °C per 30 min. After digestions, the samples were filtered with filter Whatmann n° 1 and diluted with bi-distilled water in order to reach a final concentration of HCl 0.2 M. Then, samples were newly filtered through filters Millipore (0.25 µm-pore size) and diluted for the analysis.
The ions detection and quantification were carried out by a suppressed ion chromatography, employing a Dionex DX 500 IC System (Thermo Scientific, Waltham, Massachusetts, US) equipped with a conductimeter detector (ED 40, Dionex). Cations (Na^+, NH_4^+, K^+, Mg^{2+}, Ca^{2+}) where analyzed by using an IonPack AS22 (4 X 250 mm) employing a CS12A column (4 X 250 mm), using Na_2CO_3 + $NaHCO_3$ 3.5 mM as eluent. Experiments were carried out using a flow rate of 1 mL/min.

Experimental design and statistical analysis

All the experiments were carried adopting a completely randomized design. The *in-vitro* bioassay consisted of 4 replications, raw data were fitted through a non-linear regression model using a log-logistic function (Table Curve 2d by Systat Software) in order to identify the ED_{50} parameter (Belz, Hurle, & Duke, 2005). Moreover, data means were first checked for their deviations from normality (Kolmogorov–Smirnov test), tested for

homogeneity of variances (Leven Median test) and then means were analyzed through one way ANOVA using Tukey's test ($P < 0.05$) as post-hoc.

Concerning the results on rosettes growth, stomatal density, cation and pigment content, total protein content, MDA by-product level, H_2O_2 accumulation, and chlorophyll *a* fluorescence parameters, the statistical significance of differences among the means of control and treated plants were estimated by Student's *t*-test ($P \leq 0.05$).

Metabolomic data were analyzed using the software Metaboanalyst 3.0 (http://www.metaboanalyst.ca/) (Xia et al. 2015) as previously reported by Araniti et al. (2017c). Data, expressed as metabolite concentrations, were checked for integrity and missing values were replaced with a small positive value. Data were successively normalized by the pre-added internal standard (ribitol), transformed through "Log normalization" and scaled through Pareto-Scaling. Data were then classified through Principal Component Analysis (PCA) and metabolite variations were presented as heatmap. Differences between treatments were considered significant with $P \leq 0.05$ (Student's *t*-test). Finally, the identification and visualization of the affected metabolic pathways was performed using the metaboanlyst tool MetPa (Xia et al. 2015).

2. RESULTS

2.1 Essential oils GC-MS chemical characterization

The relative abundances of the chemicals isolated from the EOs of *O. vulgare* L. ssp. *hirtum* are reported in Table 1. Forthyfive chemicals have been characterized most of which belong to the mono- and sesquiterpene classes (Table 1). In particular, 1 ester, 1 ketone, 16 monoterpenes, 12 monoterpenic alcohol, 2 monoterpenic phenol, 12 sesquiterpenes and 1 sequiterpenic alcohol have been identified.

Among them, the monoterpene o-Cymene and the two monoterpenic phenol, carvacrol and thymol, were the most abundant representing the 66.7 % of total blend.

2.2 *In-vitro* bioassay

The *in-vitro* bioassay pointed out that the EOs were characterized by a strong phytotoxic potential affecting rosettes growth and development. In fact, in seedlings treated, a statistically significant inhibition of fresh weight of rosettes (24.5 %) was observed at 32

μL/L concentration, reaching 84% of inhibition at the highest concentration (Fig. 1). The non linear regression fitting of FW raw data allowed to quantify the ED_{50}, the value of 110.9 μL/L (Fig. 1). Moreover, a reduced number of leaf development was observed in treated seedings (data not shown).

2.3 Experiments on developed seedlings of *A. thaliana*

2.3.1 Chlorophyll *a* fluorescence, pigment and protein content, lipid peroxidation and *in-situ* semi-quantitative determination of H_2O_2

Arabidopsis rosettes grown in nutrient medium enriched with essential oil were severely photoinhibited from the 6th day of the beginning of the treatment (Fig. 2). The decline of F_v/F_m increased progressively in treated seedlings from 6th day till to the end of the treatment period (Fig. 2, a). Similarly, values of Φ_{II} were severely limited at 8th and 10th days after the beginning of the treatment accompanied by the raise of both Φ_{NO} and Φ_{NPQ} values (Fig. 2, b-d).

The pseudo-color images obtained by Imaging PAM clearly confirmed the decline of both F_v/F_m and Φ_{II} parameters in full leaf blade (Fig. 3). Of note, older leaves were more compromised than younger ones and both the F_v/F_m and Φ_{II} values were lower in leaf margin than in central portion of leaf.

EOs treatment significantly affected FW, DW and DW/FW ratio (Fig. 4, a-c). In particular FW and DW were reduced by 48% and 26%, respectively (Fig. 4, a,b). On the other hand, DW/FW was significantly increased by 20% (Fig. 4, c). Moreover, EOs treatment increased the lipid peroxidation in Arabidopsis leaves, in which MDA by-product level was 24% higher than control (Fig. 4, d), and reduced significantly the total protein content of leaves by 30% (Fig. 4, e).

In addition, seedlings treated with the EOs had a lower content of photosynthetic pigments. In particular, both chlorophyll *a* and *b* content was significantly reduced by 64% and 42%, respectively. Carotenoid content was even strongly reduced by 84% by the EOs treatment (Fig. 4, f).

Finally, a high accumulation of H_2O_2 was observed in the full rosette of treated seedlings (Fig. 4, g).

2.3.2 Leaf stomatal density and stomatal size

In untreated plants stomata were open with turgid guard cells, whereas in treated plants an extremely high presence of closed stomata was observed (Fig., 5 a versus b). Moreover, EOs treatment significantly reduced, with similar amplitude, both stomatal density (~ 39% lower than control; Fig. 5, c), and size (38% lower than control; Fig. 5, d).

2.3.3 Ionomic analysis

The identification and quantification of cations through ionic chromatography pointed out significant differences between essential oil-treated and untreated seedlings (Fig. 6). Interestingly, in treated plants, a high increment in Na^+ and NH_4^+ content was observed, which was 12 and 7 folds highly concentrated than control, respectively (Fig. 6). Also K^+ (2.5 folds) and Ca^{2+} (1.8 folds) content was significantly increased in treated plants, whereas Mg^{2+} content was 0.43 folds lower than the control (Fig. 6).

2.3.4 Metabolomic GC-MS analysis on *A. thaliana*

In order to assess the effects of the EOs on Arabidopsis seedlings the data matrix, obtained through untargeted metabolomic, was analyzed through the principal component analysis (PCA). The PCA score plot (Fig. 7, A) pointed out a clear separation between treated and untreated plants. Sample separation was achieved using the first two principal components (PCs) (PC1 vs PC2) with a total variance of 81.1%, where 67.7% and 13.4% of the variance was explained by the PC1and the PC2, respectively (Fig. 7, a). The PCA loading plot (Fig. 7, a) showed that the chemicals, which allowed samples separation on PC1, were maltose, glucose, fructose, norvaline, phosphoric acid, adipic acid and threose (Fig. 7, b). On the other hand, PC2 was dominated by adipic acid, oxalic acid, indole-3-acetonitrile, acetamide and ethanolamine (Fig. 7, b). Among all the compounds isolated in Arabidopsis metabolome, significant features where identified through *t*-test analysis, which allowed to identify that 37 compounds, out of the 59 isolated, were significantly affected by the treatment. In particular, 14 amino acids, 9 organic acids, 1 fatty acid, 8 sugars, 1 sugar alcohol and 4 amines (Table 2).

Among the amino acids, which content was altered by the treatment, β-alanine was the less influenced since in treated plants its content was just a 1% higher than control. On the contrary, GABA and N-α-acetyl-L-lysine were the most affected and their content was increased by 85.8 % and 105.7 %, respectively. Similarly, L-norvaline, L-ornithine,

and putrescine content was significantly stimulated by the treatment with values ranging from 73 % to 97 % compared to the control. All the other amino acids identified were significantly reduced by EOs treatment with values ranging from 8 % (proline) to 55 % (glycine) compared to control (Table 2).

Concerning the organic acids, except to threonate, all the others were significantly reduced by the treatment. Similar trend was observed in the fatty acids and the amines isolated (Table 2). Finally, sugars content pointed out a strong reduction of sucrose (47 % lower than control), threalose (47 %), threose (75 %), mannose (5 %) and the sugar alcohol myoinositol (59 %). On the contrary, fructose (104 %), glucose (131 %) and maltose (208 %) highly accumulated in treated plants (Table 2).

A snapshot of the metabolites affected in the metabolomic network of plants exposed to EOs is reported in Fig. 8 where it is possible to observe the different regions of cell network affected by EOs. In particular, in the glycolysis pathways was observed a reduction in sucrose content and a strong increase in glucose and fructose (Fig. 8). Concerning the ascorbic acid metabolism, both myoinositol and glucuronic acid were significantly reduced, whereas an increase in threonic acid, linked to ascorbate catabolism, was observed (Fig. 8). Glyceric acid, serine, glycine and glycolic acid content, compounds linked to the 3-PGA cycle, were significantly reduced by the treatment (Fig. 8). Similarly, a significant reduction of lactic and pyruvic acids was observed, which are linked to the pyruvate cycle together with a reduction in aspartic acid and its derived amino acid lysine and an increment in β-alanine, all linked to oxaloacetic acid (Fig. 8). Concerning, the glutamate branch, linked to 2-oxoglutarate, glutamic acid, proline and urea were significantly reduced, whereas GABA, ornithine and putrescine content was incremented (Fig. 8). Finally, a significant reduction in malate was observed, suggesting a perturbation of the TCA cycle (Fig. 8).

Moreover, as reported in Fig. 9, all the identified metabolites which are involved in photorespiration were significantly inhibited by EOs treatment.

In order to evaluate the impact of EOs treatment on the biochemical pathways, the significant features were analyzed through MetPa, which is a metaboanalyst tool that combines the metabolite enrichment analysis with the topology analysis. Pathways were considered affected by the treatment only if the impact was higher than 0.2 and the data obtained are reported in Fig. 10.

The most affected pathways were related to the amino acids metabolism. Among them alanine aspartate and glutamate metabolism were the most affected (impact of 0.87)

followed by the ß-alanine metabolism, glycine, serine and threonine metabolism as well as arginine and proline metabolism on which was observed an impact ranging from 0.54 to 0.41 (Figure 10 A-B). All the others pathways identified pointed out an impact lower than 0.3 (Fig. 10 A-B).

DISCUSSION

The essential oils isolated from *O. vulgare* L. spp. *hyrtum* were mainly characterized by monoterpenes and sesquiterpenes, whose physiological effects on cell respiration, membrane integrity, plant water status, microtubule organization, have been largely reported (Araniti et al., 2017a; Araniti et al., 2017b; Grana et al., 2013). In addition, these terpenoids can act synergistically increasing their phytotoxicity (Araniti et al. 2013a).
In particular, the GC-MS analysis revealed a strong abundance of two monoterpenic phenols, namely carvacrol and thymol, and the monoterpene *o*-cymene, as already observed in wild population of *O. vulgare* from Southern Italy (De Almeida et al., 2010; Mancini et al., 2014). Their phytotoxic activity and ecological roles have been reported when isolated from the same species or subspecies of *Origanum vulgare* (de Almeida et al. 2010), and other species such as *Origanum acutidens sensu* (Kordali et al. 2008). The high abundance of these compounds makes the *O. vulgare* spp. *hyrtum* EOs of great interest for their allelopathic, phytoxic and herbicidal activity, generally linked to the presence of monoterpenes and sesquiterpenes (Amri et al., 2013).
The *in-vitro* bioassay confirmed a high phytotoxic effect of EOs on *Arabidopsis* rosettes, showing by both a strong growth reduction and extended chlorotic leaves, already at low ED_{50} value. Although, root growth was also significantly affected by EOs treatment (data not shown), the effects on rosettes were most remarkable, suggesting the aerial parts as the main target of EOs. Similar effects were already observed on *Arabidopsis* seedlings treated with the sesquiterpene *trans*-caryophyllene, which caused a root growth reduction but, above all, a stronger alterations in shoots with chlorosis and leaf deformations (Araniti et al., 2013a; Araniti et al., 2017b).

Once identified the ED_{50} concentration, the subsequent experiments were carried out on well-developed seedlings (8 days old) in order to monitor the EOs effects on the photosynthetic machinery as well as to identify the metabolic pathways affected by EOs treatment in mature leaves.

The first visible symptom of toxicity was the growth reduction of seedlings and the appearance of leaf chlorosis, at the end of treatment. These effects were associated with a relevant increase in DW/FW ratio, suggesting that seedlings are also experiencing a water status alteration. It has been reported that DW/FW increment could be partially due to an accumulation of osmoprotectants useful for intracellular osmotic adjustment (Guidi et al., 2017; Pompeiano et al., 2017) as observed in EOs-treated plants. The accumulation of osmoprotective solutes, such as putrescine, ornithine, glucose, fructose, which increased after EOs treatment, is a common response of plants when subjected to heavy metals, allelopathic or xenobiotic compounds (Sharma & Dietz, 2006). Accumulation of cytosolic compatible solutes plays a pivotal role by balancing the osmotic potential of the vacuole, where mainly inorganic ions are compartmentalized (Chaves et al., 2009; Huang et al., 2004; Handa et al., 1986). Accordingly, in *Arabidopsis* seedlings, treated with EOs, a high accumulation of Na^+, K^+, Ca^{2+} and NH_4^+ was observed.

In particular, the NH_4^+ content (8-folds higher than the control) represents the sum of both organic and inorganic nitrogen (total N) since it derived from a previous digestion of plant material and its successive acidification. However, the reduction in total protein and amino acids, in treated plants, suggests that the biggest part of the total N mainly derived from inorganic nitrogen, whose accumulation can dramatically alter plant metabolism and exacerbates the ROS production, and consequently causing oxidative damage in leaves (Tachibana et al., 1986). Furthermore, the current results suggest that the NH_4^+ accumulation together with the severe reduction in glutamate/glutamine could be attributed to an inhibition of glutamine synthetase (GS) activity, the main enzyme of ammonia assimilation pathway into organic compounds in plants (Miflin and Lea, 1976). This effect suggests that GS enzyme could be the crucial target of the *O. vulgare* spp. *hyrtum* EOs. Among the GS inhibitors, the phosphinothricin (PPT) has received special attention because of its use as a commercial herbicide, namely glufosinate (Lacuesta et al. 1992). Indeed, glufosinate, is a nonselective postemergence herbicide, largely used since 70's, that controls several grasses and broadleaf weeds (Lydon and Duke, 1999; Duke et al., 2000). Some essential oils (or some EOs bioactive components) are proficiently used as natural herbicides [for a review see (Dayan et al., 2009)], in a few case their real target is completely known. For example, cineol, an EOs chemical component, can inhibit the amino acid biosynthesis such as asparagine (Romagni et al.,

2000), but, to the best of our knowledge, no reports suggested glutamine synthase as the main target of essential oils (or some isolated compounds).

The ammonia accumulation is strictly associated with the photosynthesis rate inhibition in both C3 and C4 plants (Lacuesta et al. 1990; Wild et al. 1987). Although the metabolic changes, observed in the present study, did not indicate the photosynthetic apparatus as main target of EOs, ammonia accumulation can induce different cascade effects such as the direct inhibition of PSI and PSII reaction centers. In particular, ammonia has the ability to binds to the catalytic manganese of the oxygen-evolving complex of PSII (Britt et al., 1989) and it also reduces the pH gradient across the membrane, which can uncouple photophosphorylation (MacLachlan et al., 1994). The results indicate that chlorophyll fluorescence parameters remain unchanged until to the 6th day from the EOs treatment beginning, counteracting the effect of EOs on *Arabidopsis* seedlings. Conversely, from the 8th day onwards, the photosynthetic efficiency of PSII severely decreases in treated seedlings and a parallel increase of both Φ_{NO} and Φ_{NPQ} was observed. The Φ_{NO} usually reflects the fraction of energy, which is passively dissipated in the form of heat and fluorescence mainly due to the closed PSII, whereas Φ_{NPQ} corresponds to the fraction of energy dissipated in form of heat *via* the regulated photoprotective NPQ mechanisms, namely Δ-pH- and xanthophyll-regulated thermal dissipation (Klughammer and Schreiber 2008, Pfündel et al. 2008). So that, an increment of these coefficients suggests that excessive excitation energy can be efficiently dissipated into harmless heat and the PSII energy-regulation mechanism, this latter also supported by higher values of q_N found in treated plants. However, at saturating light intensities, a stronger enhancement of Φ_{NO} over Φ_{NPQ} reflects a suboptimal capacity of photoprotective reactions, which eventually will lead to photodamage and photoinhibition, in most cases shifting from dynamic to chronic photoinhibition (Klughammer and Schreiber 2008). For example, the oxidative stress implied by both MDA and H_2O_2 production can be partially a direct consequence of an altered ability of light processing due to the sensible increase of close reaction centers (higher values of q_L), which leads to ROS generation and propagation of oxidative stress, even at the chloroplast membrane level.

It is worth being noticed that the negative effect exerted by EOs to the photosynthetic apparatus is further exacerbated by the significant decline of the photorespiratory metabolism, which can really be helpful in plant sunder stress for several reasons (Peterhansel et al., 2010). First, photorespiration is the only pathway in the plant for

phosphoglycolate metabolism that would otherwise accumulate and inhibit key enzymes such as triose phosphate isomerase (Anderson, 1971) and phosphofructokinase (Kelly and Latzko, 1976). Second, under stressful conditions, there is an overproduction of NADPH in light reaction centers with respect to the demand of Calvin cycle and photorespiration can act as an electron sink by consuming reducing equivalents during the refixation of released ammonia and by exporting reduced components from the chloroplast to the mitochondria (Igamberdiev and Lea, 2002). Third, photorespiration can protect from photoinhibition under condition of excessive ammonia as observed in plants in which the accumulation of ammonia was obtained by manipulating the expression of glutamine synthase (Kozaki and Takeba,1996). Finally, photorespiration is obviously tightly integrated into plant primary metabolism and most of its intermediates are also part of other metabolic pathways significantly contributing to the synthesis of several amino acids (Novitskaya et al., 2002).

For the sack of the truth, beside the strong effect provoked by ammonia accumulation on plant metabolic network, there could be other further effect that have contributed to the effectiveness of *O. vulgare* EOs. For example, the strong accumulation of sodium in leaves might have markedly impaired the plant photosynthetic performance causing a decrease of the quantum yield of photosystem II and an increase of non-photochemical quenching, as also observed by other authors (Müller et al., 2014). In EOs-treated plants, a significant reduction in sucrose, which could be to both a consequence of plant reaction to oxidative stress and/or to the alterations observed on PSII, together with an increase in glucose, fructose and threonate were observed. In particular, a pronounced accumulation of threonate, which production is strictly linked to oxidative stress conditions, was observed by Obata et al (2011) in Arabidopsis plants treated with menadione (oxidative stress-inducing compound). The high threonate content, a breakdown product of ascorbate under oxidative stress (Marino et al., 2007), indicated a failure to recycle, through the ascorbate-glutathione cycle, the oxidized ascorbate, the main antioxidant compounds in the cell (Baxter *et al.*, 2007). Furthermore, it has been reported that during oxidative stress, to increase the carbon availability as energy source, plant cells increase glucose and fructose production irreversibly cleaving the sucrose through the enzymes invertases (Xiang et al., 2011). These enzymes are largely involved in protecting plants from oxidative stress (Bolouri-Moghaddam et al., 2010, Nishizawa et al., 2008; Ramel eta al., 2009; Sulmon et al., 2006). Moreover, the accumulation of these

primary metabolites was consistent with amino acids reduction linked to the downstream glycolytic intermediates and the TCA cycle.

Conclusion

The effect of *O. vulgare* spp. *hyrtum* EOs against *Arabidopsis* seedlings consisted of a series of metabolic alterations, which are likely interconnected each other: i) impairing the nitrogen assimilation into amino acids, which affects in particular the glutamine metabolism; and as consequence ii) excessive accumulation of toxic inorganic N into the leaves, associated with oxidative stress and damage; iii) declining the efficiency of the photosynthetic apparatus, connected to the reduced CO_2 fixation, which causes a plant reduction and low capacity to protect against photooxidation; iv) impairing the photorespiratory pathway therefore further exacerbating the excess of intercepted light per assimilated CO_2.

Taken together, the data highlights that EOs isolated from *Origanum vulgare* L. ssp. *hirtum* alters principally the ability of *Arabidopsis* seedlings to incorporate inorganic nitrogen into amino acids, principally glutamine, leading to a dramatic accumulation of ammonia in leaf cells. This primary effect induces, in turn, a cascade of reactions that limits the efficiency of PSII, inducing oxidative stress and finally causing a strong plant growth reduction, leaf necrosis and eventually plant death.

Acknowledgements

The research was supported by the Italian Ministry of Education, University and Research (MIUR), project SIR-2014 cod. RBSI14L9CE (MEDANAT).

Bibliography

Aktar, W., Sengupta, D., Chowdhury, A., 2009. Impact of pesticides use in agriculture: their benefits and hazards. Interdiscip. Toxicol., 2(1), 1-12.

Amri, I., Hamrouni, L., Hanana, M., & Jamoussi, B. 2013. Reviews on phytotoxic effects of essential oils and their individual components: news approach for weeds management. Int J. Appl. Biol. Pharmac. Technol., 4, 96-114.

Anderson, L. E.,1971. Chloroplast and cytoplasmic enzymes II. Pea leaf triose phosphate isomerases. Biochim. Biophys. Acta (BBA)-Enzymol., 235(1), 237-244.

Andrés, M. F., González-Coloma, A., Sanz, J., Burillo, J., Sainz, P., 2012. Nematicidal activity of essential oils: a review. Phytochem. Rev., 11(4), 371-390.

Andrés, M. F., Rossa, G. E., Cassel, E., Vargas, R. M. F., Santana, O., Díaz, C. E., González-Coloma, A., 2017. Biocidal effects of *Piper hispidinervum* (*Piperaceae*) essential oil and synergism among its main components. Food Chem. Toxicol., 109, 1086-1092.

Araniti, F., Bruno, L., Sunseri, F., Pacenza, M., Forgione, I., Bitonti, M. B., Abenavoli, M. R., 2017a. The allelochemical farnesene affects *Arabidopsis thaliana* root meristem altering auxin distribution. Plant Physiol. Bioch., 121, 14-20.

Araniti, F., Graña, E., Krasuska, U., Bogatek, R., Reigosa, M. J., Abenavoli, M. R., Sánchez-Moreiras, A. M., 2016. Loss of gravitropism in farnesene-treated *Arabidopsis* is due to microtubule malformations related to hormonal and ROS unbalance. PloS one, 11(8), e0160202.

Araniti, F., Graña, E., Reigosa, M. J., Sánchez-Moreiras, A. M., Abenavoli, M. R., 2013a. Individual and joint activity of terpenoids, isolated from *Calamintha nepeta* extract, on *Arabidopsis thaliana*. Nat. Prod. Res., 27(24), 2297-2303.

Araniti, F., Lupini, A., Sorgonà, A., Statti, G. A., Abenavoli, M. R., 2013b. Phytotoxic activity of foliar volatiles and essential oils of *Calamintha nepeta* (L.) Savi. Nat. Prod. Res., 27(18), 1651-1656.

Araniti, F., Lupini, A., Sunseri, F., Abenavoli, M. R., 2017c. Allelopatic potential of *Dittrichia viscosa* (*L.*) W. Greuter mediated by VOCs: a physiological and metabolomic approach. PloS one, 12(1), e0170161.

Araniti, F., Sánchez-Moreiras, A. M., Graña, E., Reigosa, M. J., Abenavoli, M. R., 2017b. Terpenoid trans-caryophyllene inhibits weed germination and induces plant water status alteration and oxidative damage in adult *Arabidopsis*. Plant Biol., 19(1), 79-89.

Atak, M., Mavi, K., & Uremis, I. 2016. Bio-herbicidal effects of oregano and rosemary essential oils on germination and seedling growth of bread wheat cultivars and weeds. Romanian Biotech. Lett., 21(1), 11149.

Baxter, C.J., Redestig, H., Schauer, N., Repsilber, D., Patil, K.R., Nielsen, J., Selbig, J., Liu, J., Fernie, A.R., Sweetlove, L.J., 2007. The metabolic response of heterotrophic *Arabidopsis* cells to oxidative stress. Plant Physiol., 143, 312-325.

Belz, R. G., Hurle, K., Duke, S. O., 2005. Dose-response—a challenge for allelopathy?. Nonlinearity Biol., Toxicol., Med., 3(2), nonlin-003.

Bolouri-Moghaddam, M.R., Le Roy, K., Xiang, L., Rolland, F., Van den Ende, W., 2010. Sugar signalling and antioxidant network connections in plant cells. FEBS J., 277, 2022-2037.

Bradford, M. M., 1976. A rapid and sensitive method for the quantitation of microgram quantities of protein utilizing the principle of protein-dye binding. Anal. Biochem., 72(1-2), 248-254.

Britt, R. D., Zimmermann, J. L., Sauer, K., Klein, M. P., 1989. Ammonia binds to the catalytic manganese of the oxygen-evolving complex of photosystem II. Evidence by electron spin-echo envelope modulation spectroscopy. J.Am. Chem.l Soc., 111(10), 3522-3532.

Chaimovitsh, D., Abu-Abied, M., Belausov, E., Rubin, B., Dudai, N., Sadot, E., 2010. Microtubules are an intracellular target of the plant terpene citral. Plant J., 61(3), 399-408.

Chaves, M. M., Flexas, J., Pinheiro, C., 2009. Photosynthesis under drought and salt stress: regulation mechanisms from whole plant to cell. Ann. Bot.-London, 103(4), 551-560.

Dadalio□lu, I., Evrendilek, G. A. 2004. Chemical compositions and antibacterial effects of essential oils of Turkish oregano (*Origanum minutiflorum*), bay laurel (*Laurus nobilis*), Spanish lavender (*Lavandula stoechas* L.), and fennel (*Foeniculum vulgare*) on common foodborne pathogens. J. Agricul. Food Chem., 52(26), 8255-8260.

Dayan, F. E., Cantrell, C. L., Duke, S. O., 2009. Natural products in crop protection. Bioorgan. Med. Chem., 17(12), 4022-4034.

De Almeida, L. F. R., Frei, F., Mancini, E., De Martino, L., De Feo, V., 2010. Phytotoxic activities of Mediterranean essential oils. Molecules, 15(6), 4309-4323.

De Feo, V., De Simone, F., Senatore, F. 2002. Potential allelochemicals from the essential oil of Ruta graveolens. Phytochem., 61(5), 573-578.

Dudai, N., Poljakoff-Mayber, A., Mayer, A. M., Putievsky, E., Lerner, H. R., 1999. Essential oils as allelochemicals and their potential use as bioherbicides. J. Chem. Ecol., 25(5), 1079-1089.

Duke, S. O., Dayan, F. E., Romagni, J. G., Rimando, A. M., 2000. Natural products as sources of herbicides: current status and future trends. Weed Res.-Oxford-, 40(1), 99-112.

Duke, S. O., Oliva, A., Macias, F., Galindo, J., Molinillo, J., Cutler, H., 2004. Mode of action of phytotoxic terpenoids. CRC Press: Boca Raton, FL, USA, pp. 201-206

Garcia-Rellan, D., Verdeguer, M., Salamone, A., Blázquez, M. A., Boira, H. 2016. Chemical composition, herbicidal and antifungal activity of *Satureja cuneifolia* essential oils from Spain. Nat. Prod. Commun., 11(6), 841-844.

Graña, E., Díaz-Tielas, C., López-González, D., Martínez-Peñalver, A., Reigosa, M. J., Sánchez-Moreiras, A. M., 2016. The plant secondary metabolite citral alters water status and prevents seed formation in *Arabidopsis thaliana*. Plant Biol., 18(3), 423-432.

Graña, E., Sotelo, T., Díaz-Tielas, C., Araniti, F., Krasuska, U., Bogatek, R., Sánchez-Moreiras, A. M., 2013. Citral induces auxin and ethylene-mediated malformations and arrests cell division in *Arabidopsis thaliana* roots. J. . Chem. Ecol., 39(2), 271-282.

Guidi, L., Remorini, D., Cotrozzi, L., Giordani, T., Lorenzini, G., Massai, R., Vangelisti, A., 2017. The harsh life of an urban tree: the effect of a single pulse of ozone in salt-stressed Quercus ilex saplings. Tree Physiol., 37(2), 246-260.

Handa, S., Handa, A. K., Hasegawa, P. M., Bressan, R. A., 1986. Proline accumulation and the adaptation of cultured plant cells to water stress. Plant Physiol., 80(4), 938-945.

Hodges, D. M., DeLong, J. M., Forney, C. F., Prange, R. K., 1999. Improving the thiobarbituric acid-reactive-substances assay for estimating lipid peroxidation in plant tissues containing anthocyanin and other interfering compounds. Planta, 207(4), 604-611.

Holt, J. S., Powles, S. B., Holtum, J. A., 1993. Mechanisms and agronomic aspects of herbicide resistance. Annu. Rev. Plant Biol., 4 (1), 2403-229.

Huang, X. D., El-Alawi, Y., Penrose, D. M., Glick, B. R., Greenberg, B. M., 2004. Responses of three grass species to creosote during phytoremediation. Environ. Pollut., 130(3), 453-463.

Igamberdiev, A. U., Lea, P. J., 2002. The role of peroxisomes in the integration of metabolism and evolutionary diversity of photosynthetic organisms. Phytochem., 60(7), 651-674.

Isman, M. B.,2000. Plant essential oils for pest and disease management. Crop Prot., 19(8-10), 603-608.

Kelly, G. J., Latzko, E., 1976. Inhibition of spinach-leaf phosphofructokinase by 2-phosphoglycollate. FEBS Lett., 68(1), 55-58.

Khani, A., Asghari, J., 2012. Insecticide activity of essential oils of *Mentha longifolia*, *Pulicaria gnaphalodes* and *Achillea wilhelmsii* against two stored product pests, the flour beetle, *Tribolium castaneum*, and the cowpea weevil, *Callosobruchus maculatus*. J. Insect Sci., 12(1).

Klughammer, C., Schreiber, U., 2008. Complementary PS II quantum yields calculated from simple fluorescence parameters measured by PAM fluorometry and the Saturation Pulse method. PAM Appl. Note., 1(2), 201-247.

Kordali, S., Cakir, A., Ozer, H., Cakmakci, R., Kesdek, M., Mete, E., 2008. Antifungal, phytotoxic and insecticidal properties of essential oil isolated from Turkish *Origanum acutidens* and its three components, carvacrol, thymol and p-cymene. Bioresource Technol., 99(18), 8788-8795.

Kozaki, A., Takeba, G., 1996. Photorespiration protects C3 plants from photooxidation. Nature, 384(6609), 557.

Lacuesta, M., Munoz-Rueda, A., Gonzalez-Muruá, C, Sivak, M. N. 1992. Effect of phosphlnothricin (glufosinate) on photosynthesis and chlorophyll fluorescence emission by barley leaves illuminated under photorespiratory and non-photorespiratory conditions. J. Exp. Bot., 43(2), 159-165.

Lacuesta, M., Gonzalez-Moro, B., González-Murua, C., & Munoz-Rueda, A. 1990. Temporal study of the effect of phosphinothricin on the activity of glutamine

synthetase, glutamate dehydrogenase and nitrate reductase in *Medicago sativa* L. J. plant physiol., 136(4), 410-414.

Landi, M., 2017. Commentary to:"Improving the thiobarbituric acid-reactive-substances assay for estimating lipid peroxidation in plant tissues containing anthocyanin and other interfering compounds" by Hodges et al., Planta (1999) 207: 604–611. Planta, 245(6), 1067-1067.

Lydon, J., Duke, S. O., 1999. Inhibitors of glutamine biosynthesis. Plant amino acids: Biochem. Biotechnol, 445-464.

MacLachlan, D. J., Nugent, J. H., Warden, J. T., Evans, M. C., 1994. Investigation of the ammonium chloride and ammonium acetate inhibition of oxygen evolution by Photosystem II. Biochim. Biophys. Acta (BBA)-Bioenergetics, 1188(3), 325-334.

Maherali, H., Reid, C. D., Polley, H. W., Johnson, H. B., Jackson, R. B., 2002. Stomatal acclimation over a subambient to elevated CO2 gradient in a C3/C4 grassland. Plant, Cell Environ., 25(4), 557-566.

Malone, S. R., Mayeux, H. S., Johnson, H. B., Polley, H. W.,1993. Stomatal density and aperture length in four plant species grown across a subambient CO2 gradient. Am. J. Bot., 1413-1418.

Mancini, E., Camele, I., Elshafie, H. S., De Martino, L., Pellegrino, C., Grulova, D., De Feo, V. 2014. Chemical composition and biological activity of the essential oil of *Origanum vulgare* ssp. hirtum from different areas in the Southern Apennines (Italy). Chemistry & biodiversity, 11(4), 639-651.

Marino, D., González, E.M., Frendo, P., Puppo, A., Arrese-Igor, C., 2007. NADPH recycling systems in oxidative stressed pea nodules: a key role for the NADP+-dependent isocitrate dehydrogenase. Planta, 225, 413-421.

Miflin, B. J., Lea, P. J. 1976. The pathway of nitrogen assimilation in plants. Phytochem., 15(6), 873-885

Müller, M., Kunz, H. H., Schroeder, J. I., Kemp, G., Young, H. S., Neuhaus, H. E., 2014. Decreased capacity for sodium export out of *Arabidopsis* chloroplasts impairs salt tolerance, photosynthesis and plant performance. Plant J., 78(4), 646-658.

Nishizawa, A., Yabuta, Y., Shigeoka, S., 2008. Galactinol and raffinose constitute a novel function to protect plants from oxidative damage. Plant Physiol., 147, 1251-1263.

Novitskaya, L., Trevanion, S. J., Driscoll, S., Foyer, C. H., Noctor, G., 2002. How does photorespiration modulate leaf amino acid contents? A dual approach through modelling and metabolite analysis. Plant, Cell Environ., 25(7), 821-835.

Obata, T., Matthes, A., Koszior, S., Lehmann, M., Araújo, W.L., Bock R., Sweetlove, L.J., Fernie, A.R., 2011. Alteration of mitochondrial protein complexes in relation to metabolic regulation under short-term oxidative stress in *Arabidopsis* seedlings. Phytochem., 72, 1081-1091.

Peterhansel, C., Horst, I., Niessen, M., Blume, C., Kebeish, R., Kürkcüoglu, S., Kreuzaler, F., 2010. Photorespiration. The *Arabidopsis* Book, e0130.

Pfündel, E., Klughammer, C., Schreiber, U., 2008. Monitoring the effects of reduced PS II antenna size on quantum yields of photosystems I and II using the Dual-PAM-100 measuring system. PAM Appl. Note., 1, 21-24.

Pompeiano, A., Landi, M., Meloni, G., Vita, F., Guglielminetti, L., Guidi, L., 2017. Allocation pattern, ion partitioning, and chlorophyll a fluorescence in *Arundo donax* (*L.*) in responses to salinity stress. Plant Biosyst.- Int. J. Dealing with all Aspects of Plant Biol., 151(4), 613-622.

Radoglou, K. M., Jarvis, P. G., 1990 . Effects of CO_2 enrichment on four poplar clones. II. Leaf surface properties. Ann. Bot- London, 65(6), 627-632.

Ramel, F., Sulmon, C., Bogard, M., Couée, I., Gouesbet, G., 2009. Differential patterns of reactive oxygen species and antioxidative mechanisms during atrazine injury and sucrose-induced tolerance in *Arabidopsis thaliana* plantlets. BMC Plant Biol., 9, 28.

Rolli, E., Marieschi, M., Maietti, S., Sacchetti, G., & Bruni, R. 2014. Comparative phytotoxicity of 25 essential oils on pre-and post-emergence development of *Solanum lycopersicum* L.: A multivariate approach. Ind. Crops Prod., 60, 280-290.

Romagni, J. G., Duke, S. O., Dayan, F. E., 2000. Inhibition of plant asparagine synthetase by monoterpene cineoles. Plant Physiol., 123(2), 725-732.

Sharma, S. S., Dietz, K. J., 2006. The significance of amino acids and amino acid-derived molecules in plant responses and adaptation to heavy metal stress. J. Exp. Bot., 57(4), 711-726.

Sulmon, C., Gouesbet, G., El Amrani, A., Couée, I., 2006. Sugar-induced tolerance to the herbicide atrazine in *Arabidopsis* seedlings involves activation of oxidative and xenobiotic stress responses. Plant Cell Rep., 25, 489-498.

Tachibana, K., Watanabe, T., Sekizawa, Y., Takenmatsu, T., 1986. Accumulation of ammonia in plants treated with bialaphos. J. Pestic. Sci., 11(1), 33-37.

Tworkoski, T., 2002. Herbicide effects of essential oils. Weed Sci., 50(4), 425-431.

Van Acker, F. A., Schouten, O., Haenen, G. R., van der Vijgh, W. J., Bast, A., 2000. Flavonoids can replace α-tocopherol as an antioxidant. FEBS Lett., 473(2), 145-148.

Verdeguer, M., García-Rellán, D., Boira, H., Pérez, E., Gandolfo, S., Blázquez, M. A. 2011. Herbicidal activity of *Peumus boldus* and *Drimys winterii* essential oils from Chile. Molecules, 16(1), 403-411.

Vrbničanin, S., Pavlović, D., Božić, D., 2017 .Weed Resistance to Herbicides. In Herbicide Resistance in Weeds and Crops. InTech.

Wellburn, A. R., 1994. The spectral determination of chlorophylls a and b, as well as total carotenoids, using various solvents with spectrophotometers of different resolution. J. Plant Physiol., 144(3), 307-313.

Xia, J., Sinelnikov, I. V., Han, B., Wishart, D. S., 2015. MetaboAnalyst 3.0—making metabolomics more meaningful. Nucleic Acids Res., 43(W1), W251-W257.

Xiang, L., Le Roy, K., Bolouri-Moghaddam, M.-R., Vanhaecke, M., Lammens, W., Rolland, F., Van den Ende ,W., 2011. Exploring the neutral invertase–oxidative stress defence connection in *Arabidopsis thaliana*. J. Exp. Bot., 62(11), 3849-3862.

Table 1: GC-MS chemical characterization of *Origanum vulgare* ssp. *hirtum* essential oils.

Apex RT	Compound	%Area	Classes
4.43	Methyl-2-methylbutanoate	0.12	Ester
9.9	α-Thujene	0.04	Monoterpenes
10.07	α-Pinene	0.76	Monoterpenes
10.5	Camphene	0.08	Monoterpenes
11.2	ß-Pinene	0.08	Monoterpenes
11.33	Morillol	0.16	Monoterpenic alchool
11.45	Octan-3-one	0.06	ketone
11.54	ß-Myrcene	0.98	Monoterpenes
11.77	Sabinene	0.03	Monoterpenes
11.88	Δ-3-Carene	0.11	Monoterpenes
11.99	α-Terpinene	0.38	Monoterpenes
12.14	o-Cymene	19.79	Monoterpenes
12.2	Limonene	1.04	Monoterpenes
12.24	Eucalyptol	0.27	Monoterpenes
12.34	ß-Ocimene	0.02	Monoterpenes
12.65	γ-Terpinene	0.06	Monoterpenes
12.78	*trans*-4-Thujanol	0.09	Monoterpenic alchool
13.18	Linalool	2.86	Monoterpenic alchool
13.46	*trans*-p-2-Menthen-1-ol	0.04	Monoterpenic alchool
13.61	1-Terpinenol	0.03	Monoterpenic alchool
13.67	*cis*-2-p-Menthen-1-ol	0.03	Monoterpenic alchool
13.73	Myrtenol	0.05	Monoterpenic alchool
13.97	Borneol	0.46	Monoterpenic alchool
14.07	4-Terpineol	2.36	Monoterpenic alchool
14.14	p-Cymen-8-ol	0.2	Monoterpenic alchool
14.2	α-Terpineol	1.02	Monoterpenic alchool
14.25	Carvone	0.1	Monoterpenes
14.33	α-phellandrene	0.05	Monoterpenes
14.56	3-methoxy-p-Cymene	1.63	Monoterpenes
14.99	3-p-Cymenol	0.92	Monoterpenic alchool
15.06	Thymol	27.19	Monoterpenic phenol
15.14	Carvacrol	19.15	Monoterpenic phenol
15.72	Ylangene	0.15	Sesquiterpenes
15.75	α-Copaene	0.32	Sesquiterpenes
16.1	ß-Caryophyllene	0.68	Sesquiterpenes
16.13	α-Bergamotene	0.11	Sesquiterpenes

16.23	Aromadendrene	0.1	Sesquiterpenes
16.33	α-Humulene	0.24	Sesquiterpenes
16.45	γ-Muurolen	4.7	Sesquiterpenes
16.71	ß-Bisabolene	0.97	Sesquiterpenes
16.74	Δ-Cadinene	2.01	Sesquiterpenes
16.86	α-Muurolen	0.16	Sesquiterpenes
16.92	α-Calacorene	0.15	Sesquiterpenes
17.64	Cadinol	0.19	Sesquiterpenic alchool
17.94	Guaiazulene	0.23	Sesquiterpenes

Table 2. List of the metabolites, identified and quantified trough GC-MS, significantly affected in Arabidopsis seedlings exposed to *O. vulgare* ssp. *Hirtum* essential oils (110.9 µL/L). Data are expressed in nanograms/100mg of fresh plant material.

Metabolite	Control	Treated	%		*P* value	Classes
GABA	18.98	35.27	85.82	↑	0.00014394	
Glutamic acid	291.02	150.57	48.26	↓	0.0480	
Glycine	58.29	26.10	55.22	↓	0.000127	
L-Asparagine	163.64	133.76	18.26	↓	0.041173	
L-Aspartic acid	161.10	88.09	45.32	↓	0.0035096	
L-Glutamine	495.84	379.19	23.52	↓	0.044743	
L-Lysine	9.44	8.23	12.82	↓	0.0035077	**Amino acids**
L-Norvaline	1.04	2.05	97.11	↑	0.014	
L-Ornithine	55.49	92.21	66.17	↑	0.0337	
L-Proline	55.15	50.61	8.23	↓	0.00060967	
N-α-acetyl-L-lysine	7.11	14.63	105.76	↑	0.00099775	
Putrescine	20.36	35.27	73.23	↑	0.0229	
Serine	319.41	159.44	50.08	↓	0.00322	
D-Gluconic acid	19.69	18.31	7.01	↓	0.00023667	
D-Glucuronic acid	59.13	55.82	5.59	↓	0.00038964	
Glyceric acid	5.18	3.85	25.72	↓	0.0234	
Glycolic acid	6.78	2.90	57.22	↓	0.0066977	
Lactic acid	80.75	32.87	59.29	↓	0.0013261	**Organic acids**
Malic acid	95.01	35.47	62.67	↓	0.0115	
Phosphoric acid	752.29	98.43	86.91	↓	0.000137	
Pyruvic acid	1.87	0.86	54.01	↓	0.0056863	
Threonate	14.97	15.79	5.48	↑	0.0026412	
Palmitic acid	64.41	33.41	48.13	↓	0.033578	**Fatty acids**
α-D-Mannopyranose	12.86	13.18	2.49	↑	0.0180	
Glucose	72.73	167.77	130.67	↑	0.0186	
Threose	51.55	12.83	75.11	↓	0.0204	
Sucrose	692.13	365.17	47.24	↓	0.0011286	**Sugars**
Threalose	155.26	82.33	46.97	↓	0.0056548	
D-Mannose	419.93	398.38	5.13	↓	0.0003614	
Maltose	13.64	42.02	208.06	↑	0.00375	
Fructose	115.44	235.29	103.82	↑	0.00498	
Myoinositol	289.62	118.10	59.22	↓	0.0311	**Sugar alcohol**
Ethanolamine	4.60	2.16	53.04	↓	0.044184	**Amine**
Hydroxylamine	107.28	61.04	43.1	↓	0.011846	

Urea	15.52	6.65	57.15	↓	0.028829
N-Acetyl-D-glucosamine	69.68	34.02	51.18	↓	0.031572

Figure 1: Dose–response curves of aerial part biomass of *Arabidopsis thaliana* seedlings exposed to increasing doses of essential oils extracted from a Calabrian wild population of *Origanum vulgare* ssp. *hirtum*. FW: fresh weight. ED_{50}: dose causing 50% reduction of total plant biomass with respect to control seedlings. N=4.

Fig. 2: Values of (a) maximum quantum efficiency of photosystem II (PSII) in dark-adapted conditions (F_v/F_m), (b) PSII operating efficiency (Φ_{II}), quantum yield of regulated (Φ_{NPQ}), and (c) nonregulated energy dissipation of PSII (Φ_{NO}), (d) coefficient of non-photochemical quenching (q_N) and (e) fraction of PSII centers that are 'open' based on the lake model of PSII (q_L) in *Arabidopsis* seedlings exposed or not to *Origanum vulgare* ssp. *hirtum* essential oil (110.9 µL/L). Measurements were carried out every two days from the beginning of the treatment (day 0) to ten days after (day 10). Fifteen measures were obtained for each parameter at each measuring time, which gave a kinetic plot for each parameter along the time. The integral value of the area was obtained from for each parameter at every time. * $P < 0.05$; ** $P < 0.01$; *** $P < 0.001$. AU = Arbitrary Unit. N = 3.

Fig 3: Representative pseudo-colour images of photosystem II (PSII) maximum quantum efficiency of (F_v/F_m) [a (control) and b (treated)] and PSII operating efficiency (Φ_{II}) [c (control) and d (treated)] in *Arabidopsis* seedlings exposed (or not) to *Origanum vulgare* ssp. *hirtum* essential oils for 10 days (110.9 µL/L). Images are depicted in false colors coding from 0.0 (black) to 1.0 (purple).

Fig. 4: Fresh weight (FW; a), dry weight (DW; b), DW/FW (c), total protein content (d), level of malondialdheyede by-products (e), pigments content (f) and *in-situ* semi-quantitative determination of H_2O_2 (g) evaluated on *Arabidopsis* seedlings exposed to *Origanum vulgare* ssp. *hirtum* essential oils (110.9 µL/L). Data are expressed as percentage compared to control. Asterisks indicate significant differences between mean values of treated and control plants after *t*-test with $P \leq 0.05$: * ($P \leq 0.05$), ** ($P \leq 0.01$), *** ($P \leq 0.001$). N=4.

Fig. 5: Effects of the essential oils of *Origanum vulgare* ssp. *hirtum* essential oils (10 days; 110.9 µL/L) on stomatal density and size of developed seedlings of *Arabidopsis*. Micrographs of control a) and b) treated leaf. c) stomatal density, d) stomatal size. Asterisks indicate significant differences between mean values (n=4) of treated and control plants after *t*-test with $P \leq 0.05$: * ($P \leq 0.05$), ** ($P \leq 0.01$), *** ($P \leq 0.001$). Magnification 4X (a) and 10X (b), scale bar 20 µm. N=4.

Fig. 6: Cationic content evaluated through ionic chromatography on seedlings exposed to *Origanum vulgare* ssp. *Hirtum* essential oils (110.9 µL/L). Data are expressed as percentage variation as compared to control (assuming 100%). To increase the visibility of the differences among ions content the Y axes has been presented in a Log scale. Asterisks indicate significant differences between mean values (n=4) of treated and control plants after *t*-test with $P \leq 0.05$: * ($P \leq 0.05$), ** ($P \leq 0.01$), *** ($P \leq 0.001$). N=3.

Fig 7: PCA analysis carried on the metabolite identified and quantified in *A. thaliana* rosettes exposed to *O. vulgare* ssp. *Hirtum* essential oils (110.9 µL/L). A) Principal Component Analysis model scores-plot and B) loading plot of metabolite profile of control plants (Control-1 – Contr-4, replicates of control samples) and plants exposed to *essential oils treatment* (Treated-1 – Treated-4, replicates of the treated samples). Both score and loading plots were generated using the first two PCs, PC1 *vs* PC2, with the explained variances shown in brackets. N=4.

Fig. 8: Schematic representation of the qualitative changes in metabolite content, in seedlings exposed to *Origanum vulgare* ssp. *hirtum* essential oils (110.9 µL/L), onto the

metabolic network. Solid arrows indicate a single step reaction connecting two metabolites, whereas dashed arrows multiple steps. Metabolites labeled in yellow indicate no significant change, in green a significant increase and in red significant reduction of their content. Changes were statistically analyzed through *t*-test with $P \leq 0.05$. Metabolites labeled in grey color indicate unmeasured metabolites.

Fig. 9: Effects of the essential oils of *Origanum vulgare* ssp. *hirtum* (110.9 µL/L) on the photorespiratory metabolism of developed seedlings of *Arabidopsis*. 2-OG, 2-oxoglutarate; Glu, glutamic acid; Gln, glutamine; OAA, oxaloacetate; RuBp, Ribulose 1,5-bisphosphate.

Fig. 10: Result from "*Pathway Analysis*" carried on the concentrations of metabolite identified in Arabidopsis seedlings exposed to *Origanum vulgare* ssp. *hirtum* essential oils (110.9 µL/L). A) Summary of pathway analysis carried out with MetPa; B) Results from ingenuity pathway analysis with MetPa. Total Cmpd: the total number of compounds in the pathway; Hits: is the actually matched number from the uploaded data; -Log(P) value: is the logarithm of the original p value calculated from the enrichment analysis; Impact: is the pathway impact value calculated from pathway topology analysis.

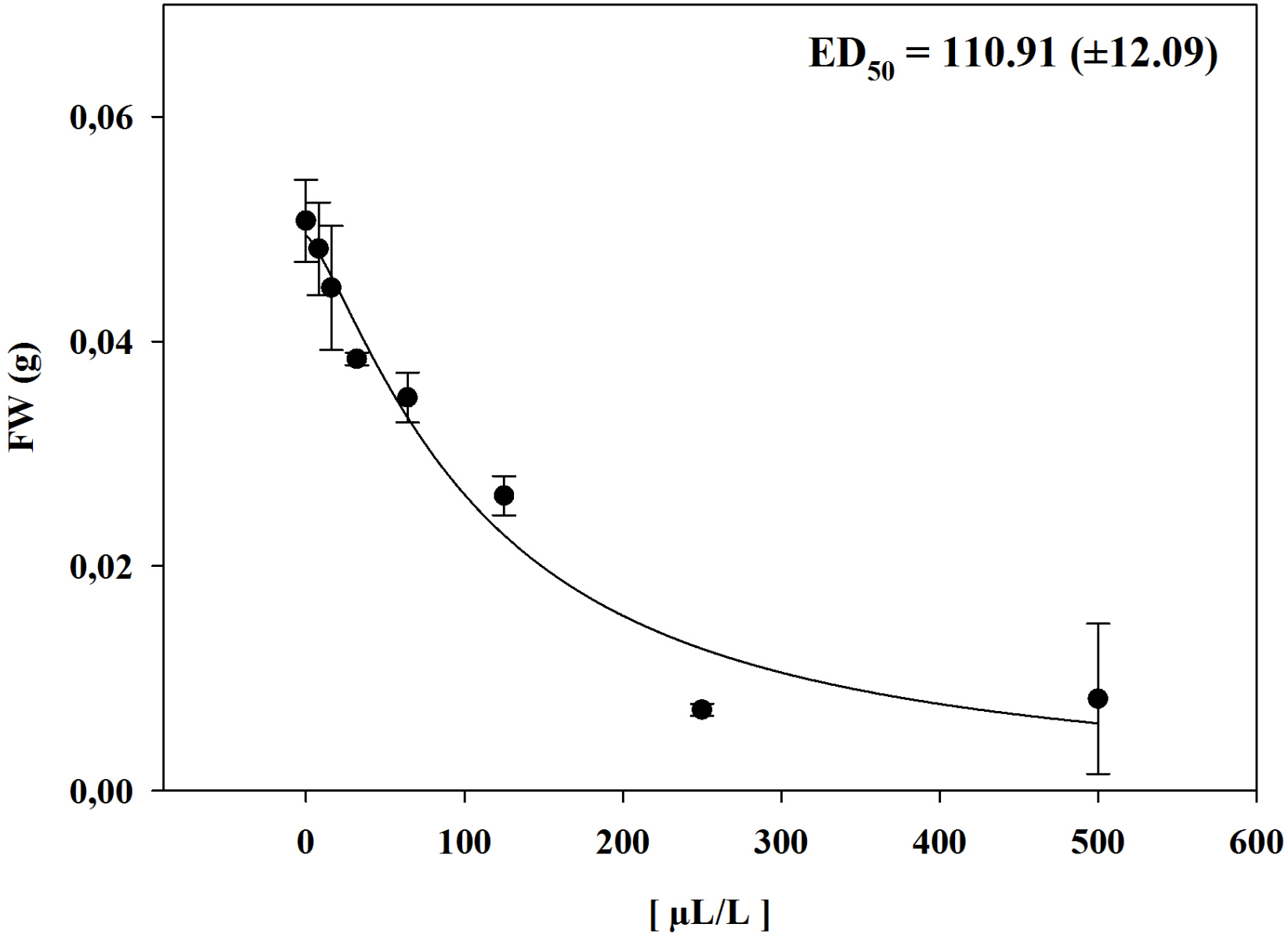
ED50 = 110.91 (±12.09)
0,06
0,04
0,02
0,00
FW (g)
0
100
200
300
400
500
600
[µL/L]

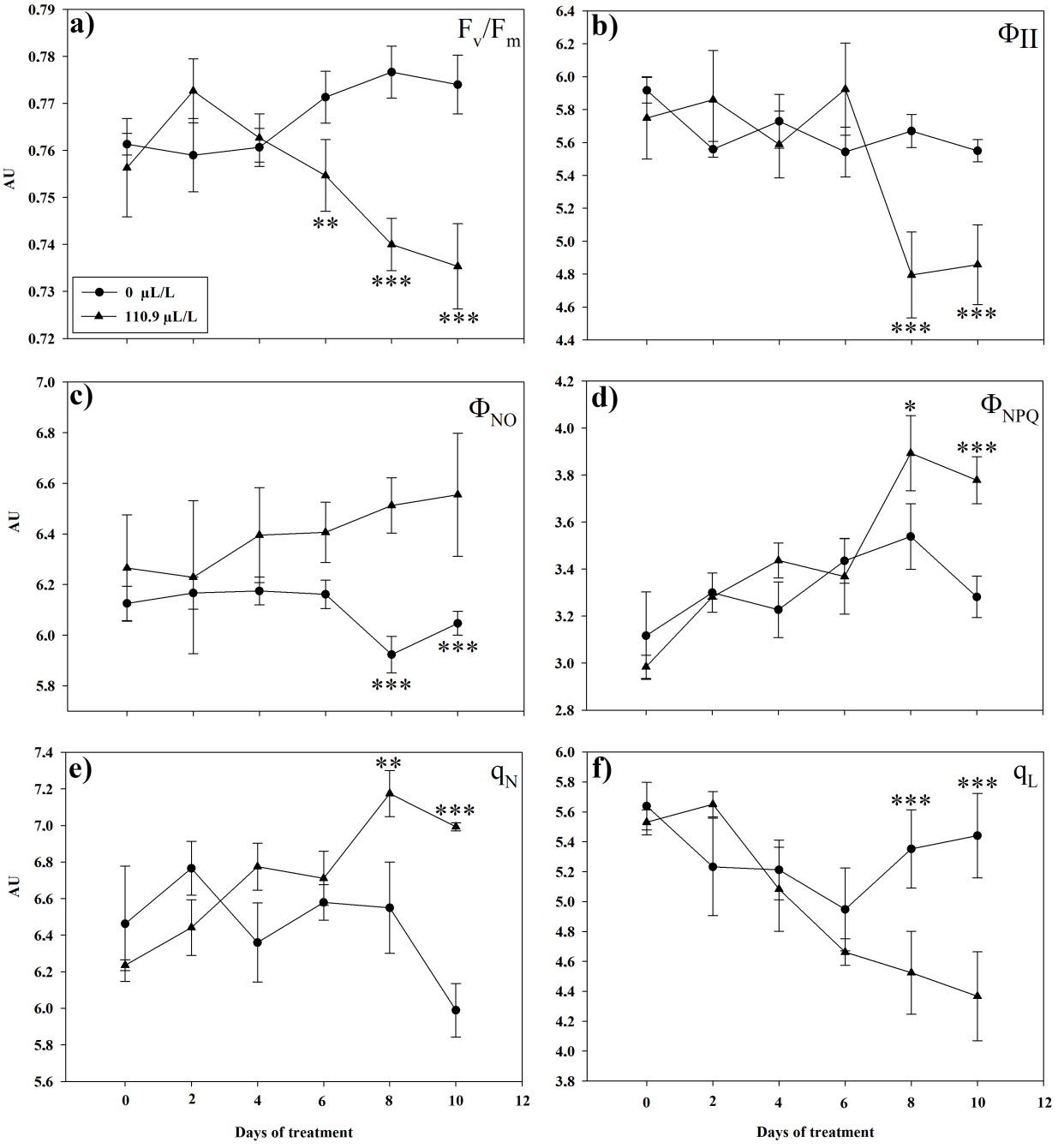
a)
F_v/F_m
b)
Φ_{II}
c)
Φ_{NO}
d)
Φ_{NPQ}
e)
q_N
f)
q_L
AU
0 µL/L
110.9 µL/L
Days of treatment
Days of treatment

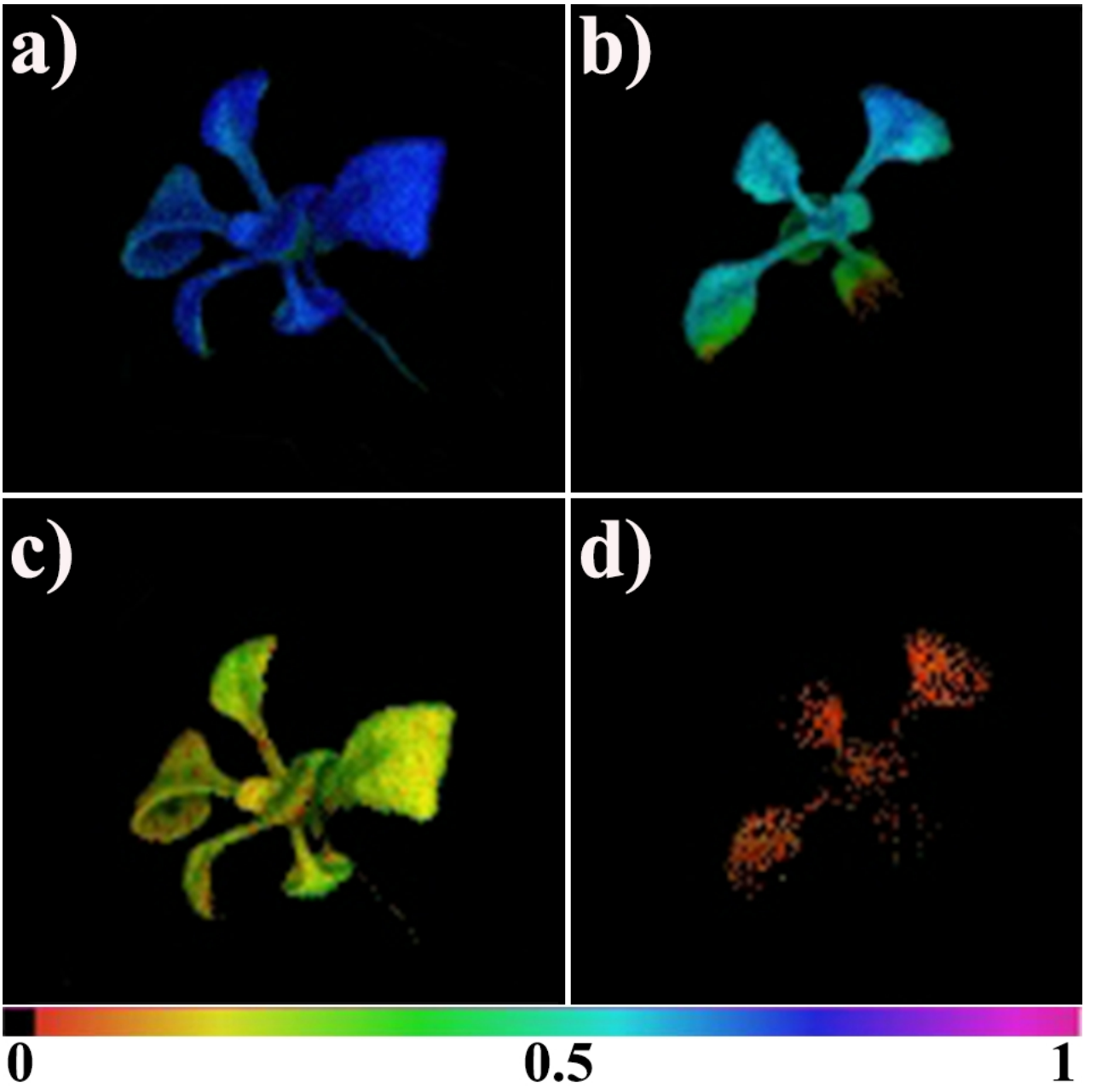
a)
b)
c)
d)
0
0.5
1

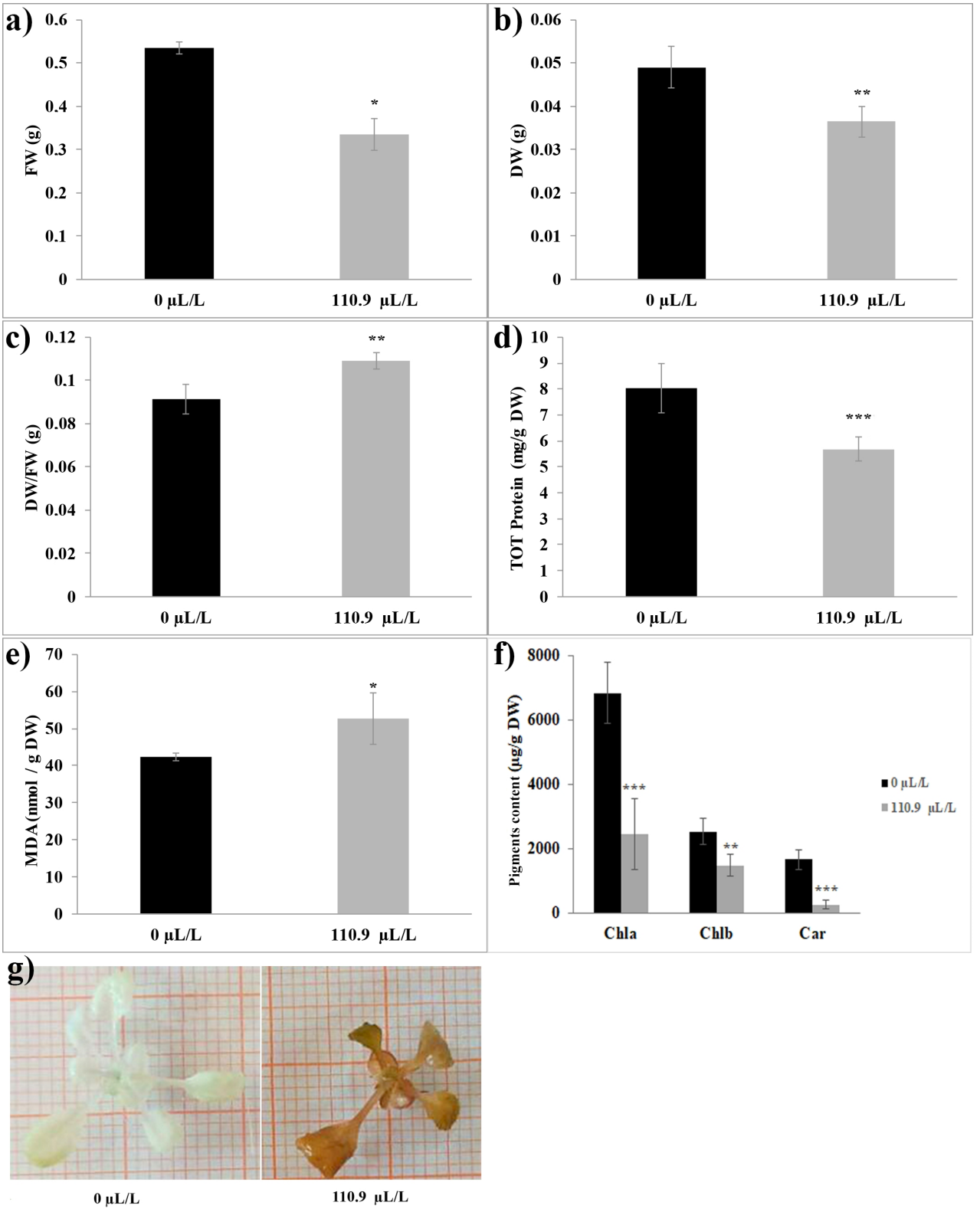
a)
FW (g)
0.6
0.5
0.4
0.3
0.2
0.1
0
*
0 µL/L
110.9 µL/L
b)
DW (g)
0.06
0.05
0.04
0.03
0.02
0.01
0
**
0 µL/L
110.9 µL/L
c)
DW/FW (g)
0.12
0.1
0.08
0.06
0.04
0.02
0
**
0 µL/L
110.9 µL/L
d)
TOT Protein (mg/g DW)
10
9
8
7
6
5
4
3
2
1
0
***
0 µL/L
110.9 µL/L
e)
MDA (nmol / g DW)
70
60
50
40
30
20
10
0
*
0 µL/L
110.9 µL/L
f)
Pigments content (µg/g DW)
8000
6000
4000
2000
0
***
**
***
Chla
Chlb
Car
0 µL/L
110.9 µL/L
g)
0 µL/L
110.9 µL/L

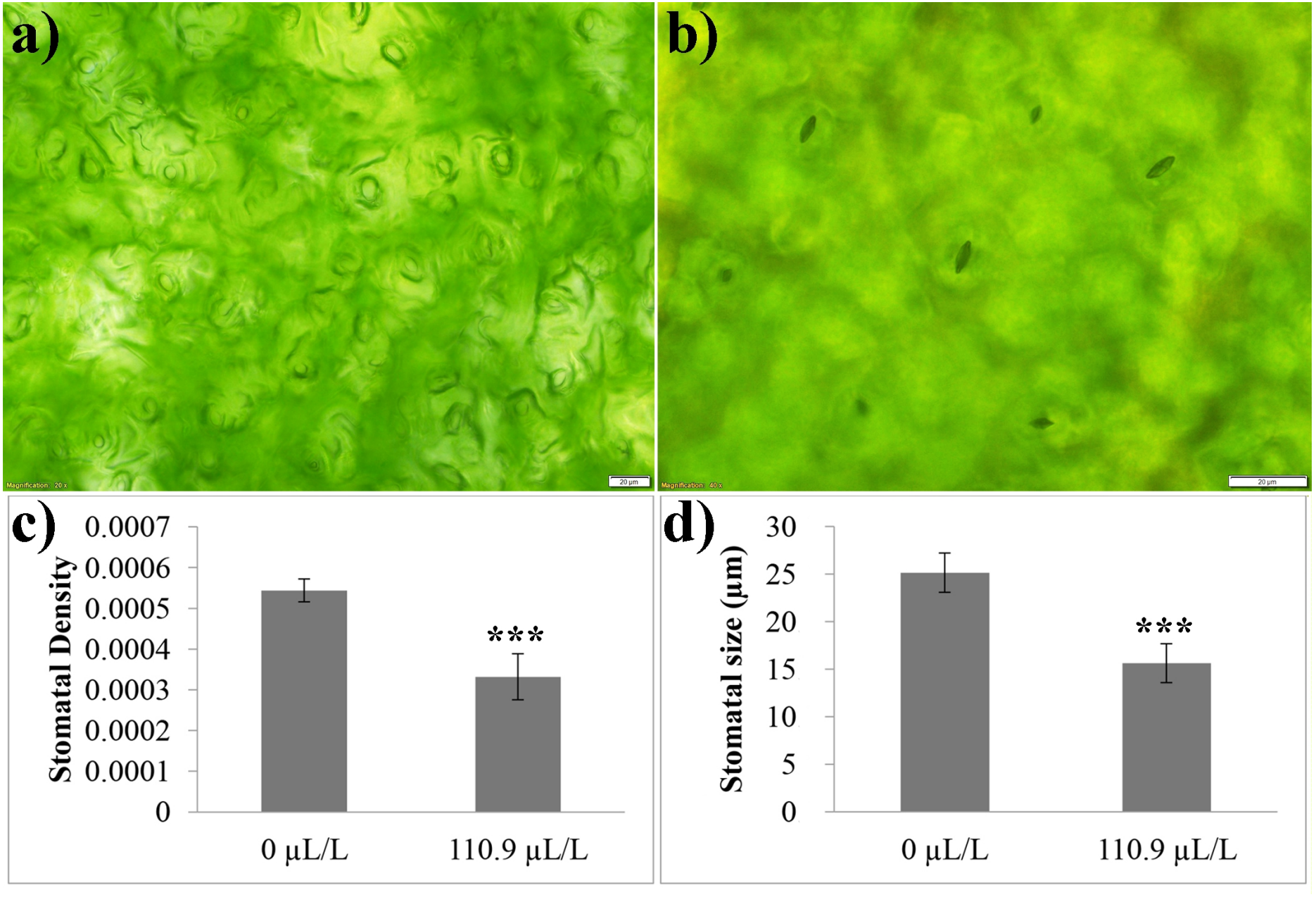
a)
b)
c)
Stomatal Density
0.0007
0.0006
0.0005
0.0004
0.0003
0.0002
0.0001
0
***
0 µL/L
110.9 µL/L
d)
Stomatal size (µm)
30
25
20
15
10
5
0
***
0 µL/L
110.9 µL/L

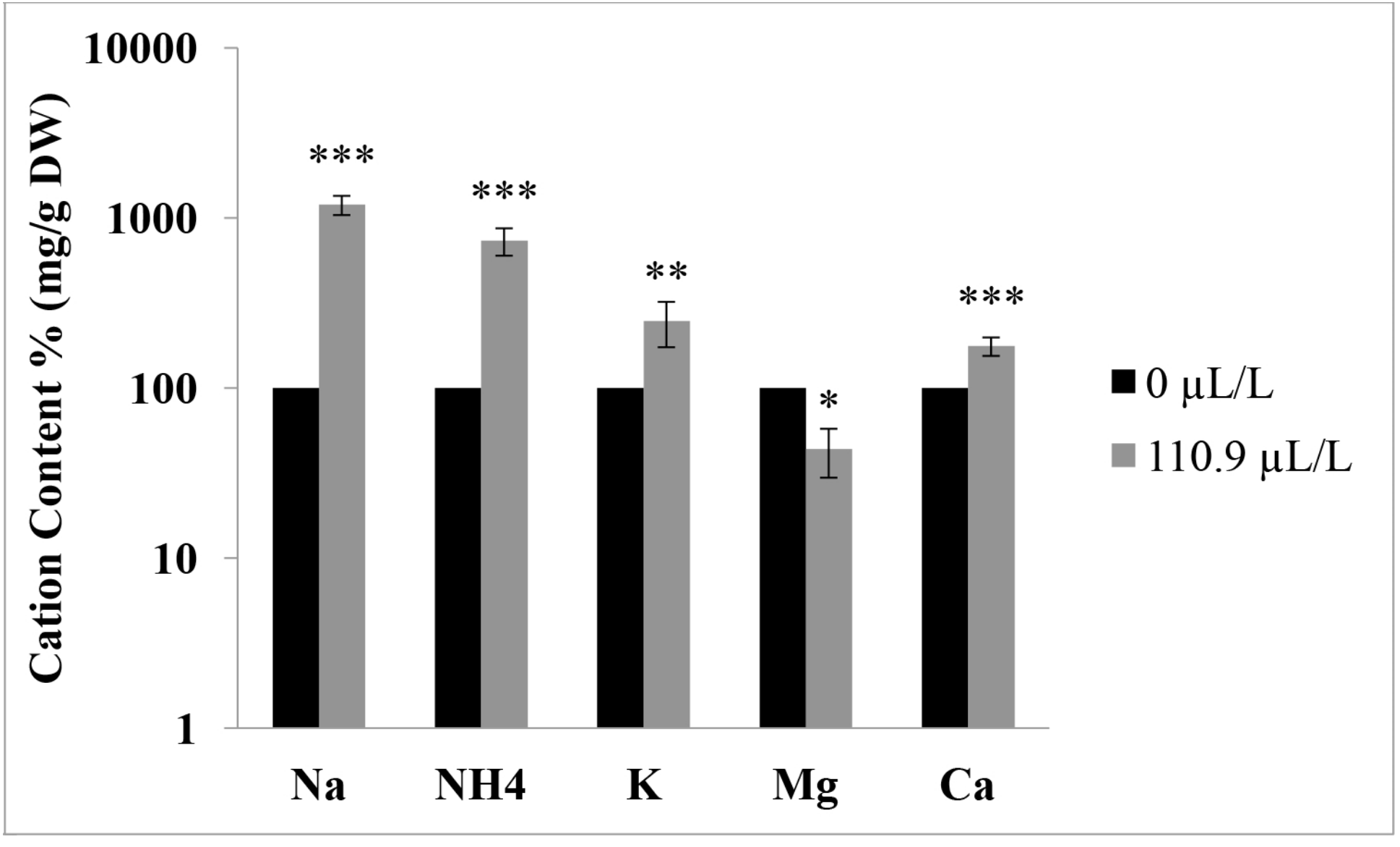
10000
1000
100
10
1
Cation Content % (mg/g DW)
***
***
**
*
***
Na
NH4
K
Mg
Ca
0 µL/L
110.9 µL/L

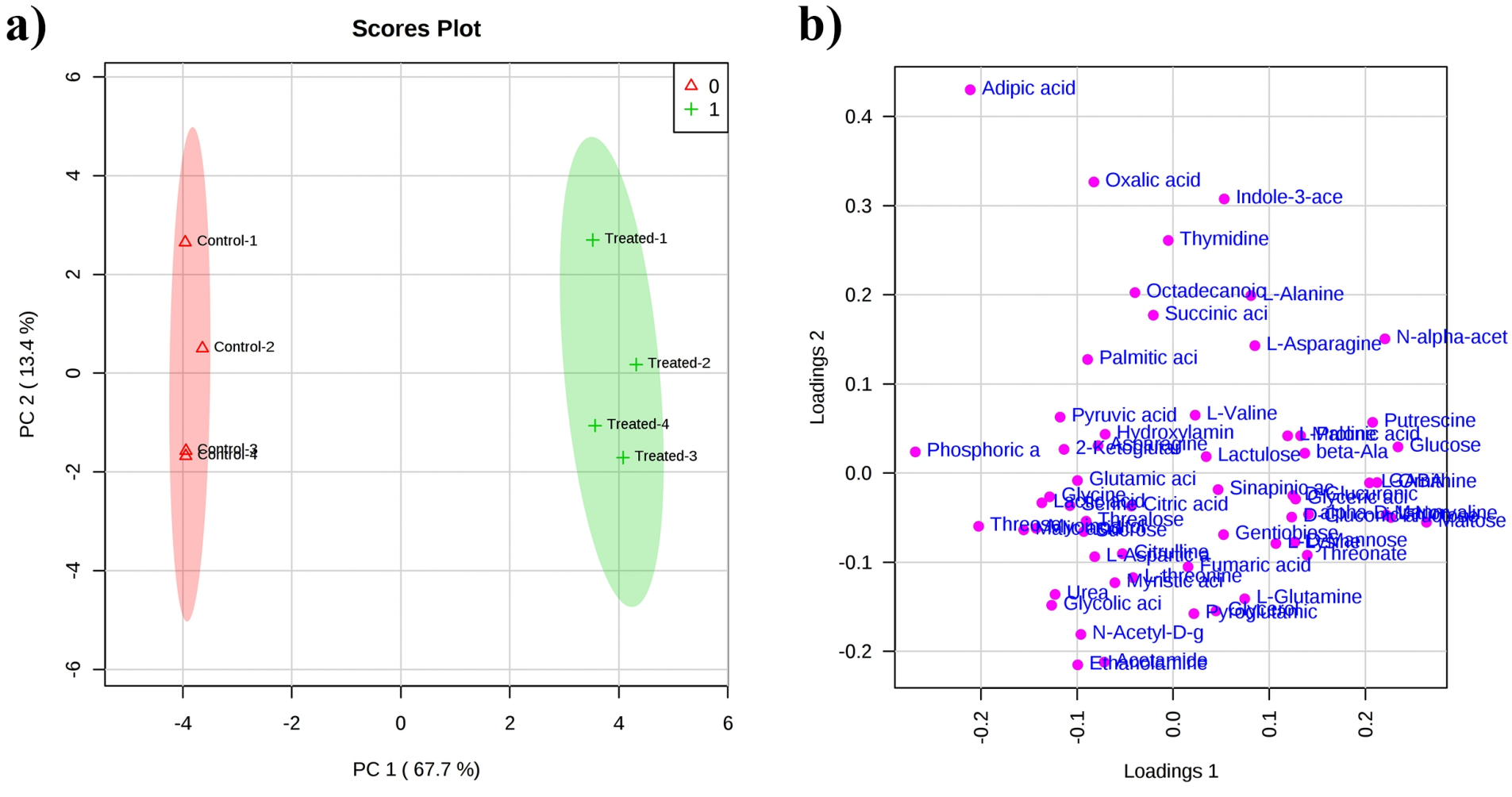
a)
Scores Plot
0
1
Control-1
Control-2
Control-3
Control-4
Treated-1
Treated-2
Treated-3
Treated-4
PC 2 (13.4 %)
PC 1 (67.7 %)
b)
Adipic acid
Oxalic acid
Indole-3-ace
Thymidine
Octadecanoic
L-Alanine
Succinic aci
L-Asparagine
N-alpha-acet
Palmitic aci
Pyruvic acid
L-Valine
Putrescine
Hydroxylamin
Phosphoric a
2-Ketoglutar
Lactulose
beta-Ala
Glucose
Glutamic aci
Sinapinic ac
Glycine
Citric acid
Threalose
Gentiobiose
Threonate
L-Aspartic a
Fumaric acid
Urea
Myristic aci
L-Glutamine
Glycolic aci
N-Acetyl-D-g
Ethanolamine
Loadings 2
Loadings 1

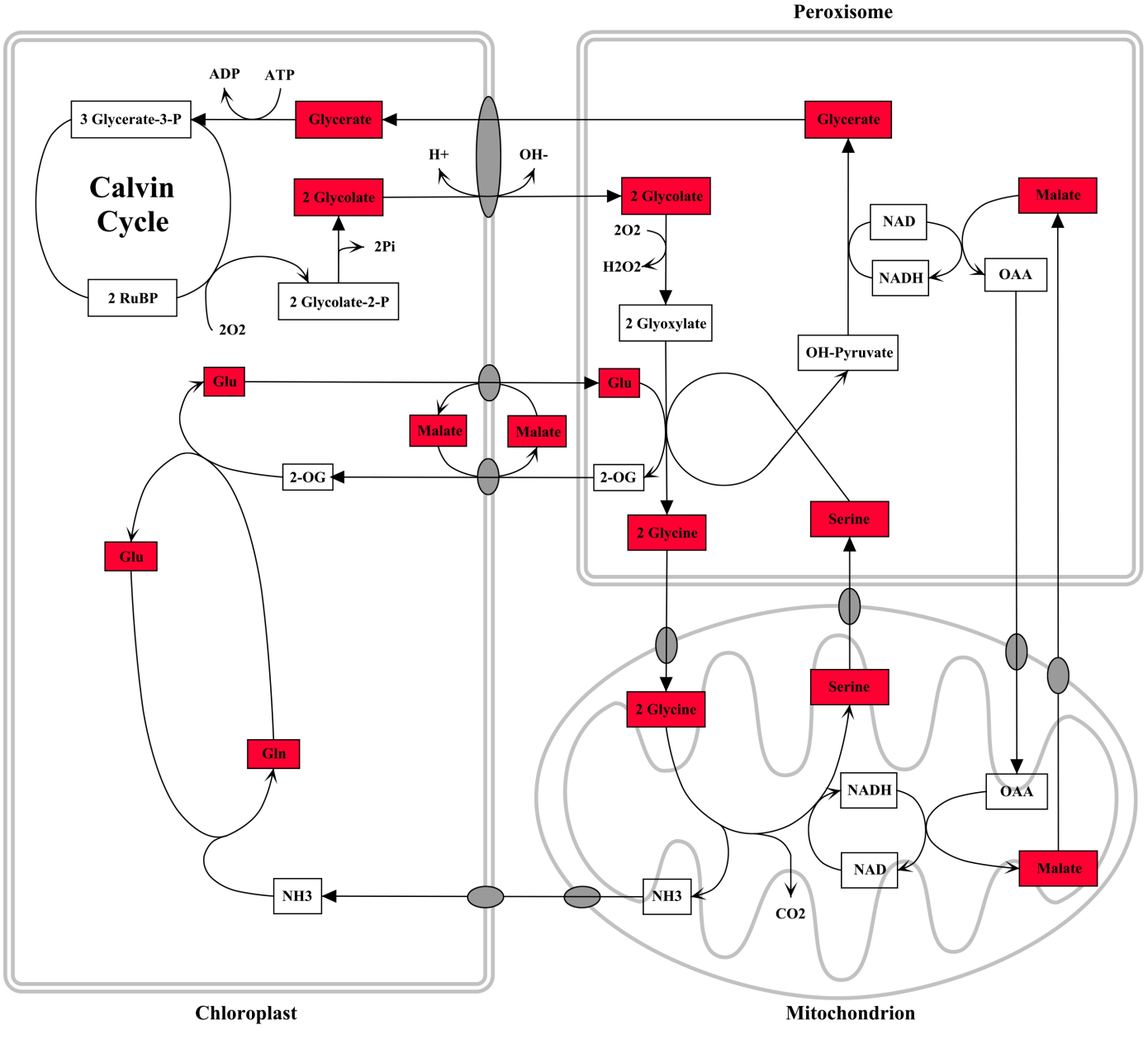
Peroxisome
ADP
ATP
3 Glycerate-3-P
Glycerate
Glycerate
Calvin Cycle
H+
OH-
2 Glycolate
2 Glycolate
2Pi
2 RuBP
2 Glycolate-2-P
2O2
2O2
H2O2
2 Glyoxylate
NAD
NADH
Malate
OAA
OH-Pyruvate
Glu
Glu
Malate
Malate
2-OG
2-OG
2 Glycine
Serine
Glu
Gln
2 Glycine
Serine
NADH
OAA
NAD
Malate
NH3
NH3
CO2
Chloroplast
Mitochondrion

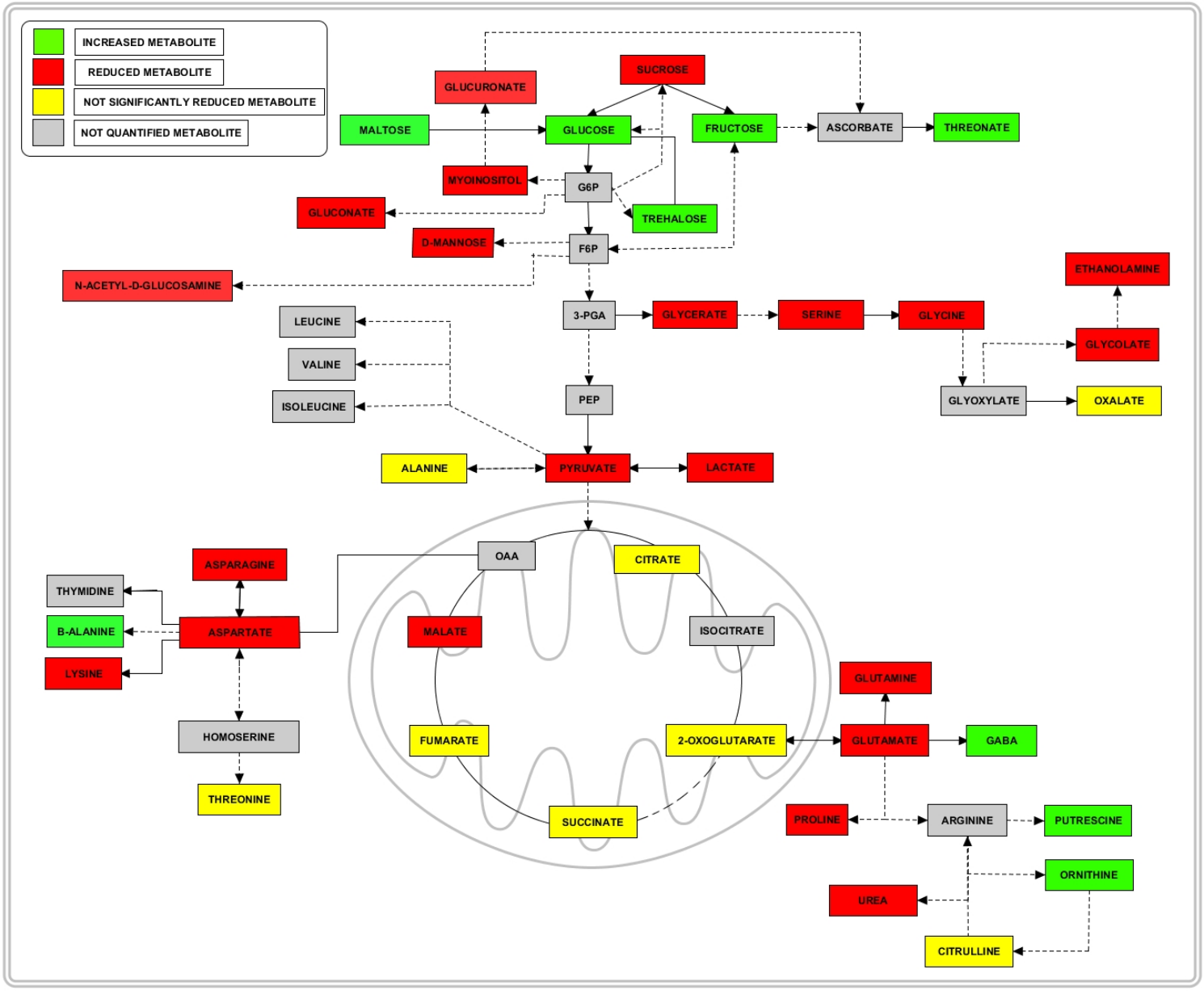
INCREASED METABOLITE
REDUCED METABOLITE
NOT SIGNIFICANTLY REDUCED METABOLITE
NOT QUANTIFIED METABOLITE
SUCROSE
GLUCURONATE
MALTOSE
GLUCOSE
FRUCTOSE
ASCORBATE
THREONATE
MYOINOSITOL
G6P
GLUCONATE
TREHALOSE
D-MANNOSE
F6P
N-ACETYL-D-GLUCOSAMINE
ETHANOLAMINE
LEUCINE
3-PGA
GLYCERATE
SERINE
GLYCINE
VALINE
GLYCOLATE
ISOLEUCINE
PEP
GLYOXYLATE
OXALATE
ALANINE
PYRUVATE
LACTATE
ASPARAGINE
OAA
CITRATE
THYMIDINE
B-ALANINE
ASPARTATE
MALATE
ISOCITRATE
LYSINE
GLUTAMINE
HOMOSERINE
FUMARATE
2-OXOGLUTARATE
GLUTAMATE
GABA
THREONINE
SUCCINATE
PROLINE
ARGININE
PUTRESCINE
ORNITHINE
UREA
CITRULLINE

a)

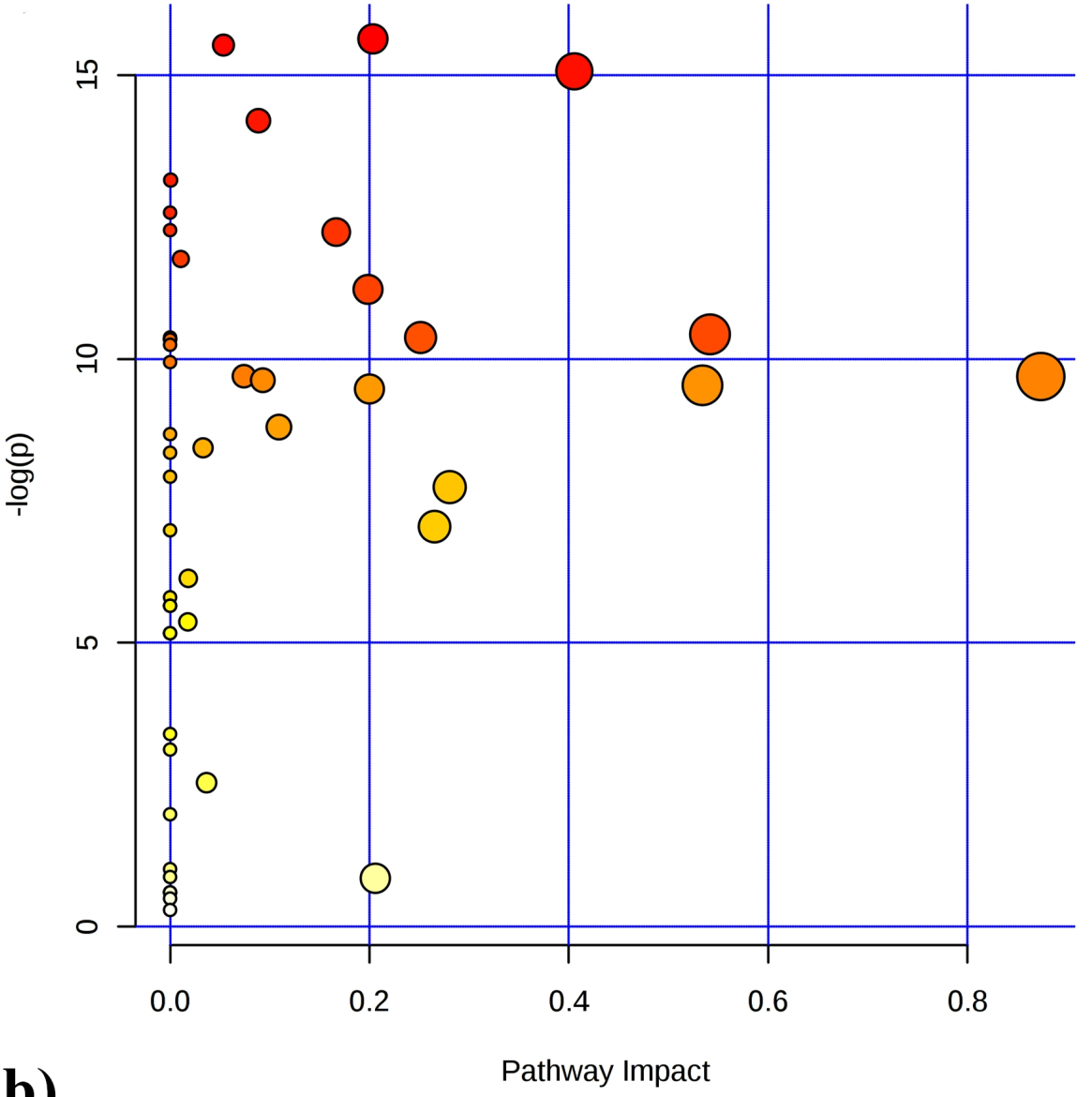

b)

Pathways	Total Cmpd	Hits	-Log(p)	Impact
Alanine aspartate and glutamate metabolism	22	10	9.69	0.87
beta-Alanine metabolism	12	2	10.43	0.54
Glycine serine and threonine metabolism	30	5	9.53	0.53
Arginine and proline metabolism	38	10	15.06	0.41
Citrate cycle (TCA cycle)	20	6	7.74	0.28
Glyoxylate and dicarboxylate metabolism	17	4	7.05	0.27
Inositol phosphate metabolism	24	1	10.38	0.25
Tryptophan metabolism	27	1	0.85	0.21
Starch and sucrose metabolism	30	5	15.64	0.20
Pantothenate and CoA biosynthesis	14	3	9.47	0.20
Pyruvate metabolism	21	3	11.23	0.20